بسم الله الرحمن الرحيم

Department of Electrical and Electronic Engineering (EEE)

ISLAMIC UNIVERSITY OF TECHNOLOGY
(IUT)

A Brief Study of Nanowire FET Biosensor and Analysis of Electrical Properties of Si and ZnO Gate-all-around Nanowire FET

BY

SYED ZAHIN REZA (122470)
MD. SHAHRUL ISLAM (122474)

SUPERVISED BY
DR. SYED IFTEKHAR ALI
Associate Professor

A Thesis Submitted to the Academic Faculty in Partial Fulfilment of the Requirements for the Degree of

Department of Electrical and Electronic Engineering (EEE)
ISLAMIC UNIVERSITY OF TECHNOLOGY (IUT)
November, 2016

DECLARATION OF CANDIDATE

It is hereby declared that the work reported in the B.Sc. thesis entitled "**A Brief Study of Nanowire FET Biosensor and Analysis of Electrical Properties of Si and ZnO Gate-all-around Nanowire FET**" submitted at **Islamic University of Technology (IUT),** Board Bazar, Gazipur, Bangladesh, is an authentic record of our work carried out under the supervision of **Prof. Dr. Syed Iftekhar Ali**. We have not submitted this work elsewhere for any other degree or diploma.

Syed Zahin Reza
Student No. 122470
Academic Year: 2015-2016
Date: 10 November, 2016

Md. Shahrul Islam
Student No. 122474
Academic Year: 2015-2016
Date: 10 November, 2016

Approved By

Dr. Mohammad Ashraful Hoque
Professor and Head of the department,
Department of Electrical and Electronic Engineering,
Islamic University of Technology (IUT),
Boardbazar, Gazipur-1704.
Date: 10 November, 2016

Supervised By

Dr. Syed Iftekhar Ali
Supervisor and Associate Professor,
Department of Electrical and Electronic Engineering,
Islamic University of Technology (IUT),
Boardbazar, Gazipur-1704.
Date: 10 November, 2016

Table of Contents

List of Tables

List of Figures

List of Acronyms

NEMS	Nano-electro-mechanical system
SQUID	Super Conductive Quantum Interference Device
DNA	Deoxy Ribonucleic Acid
CNT	Carbon Nanotube
CMOS	Complementary Metal Oxide Semiconductor
FET	Field Effect Transistor
Si-NW	Silicon Nanowire
CVD	Chemical Vapor Deposition
SOI	Silicon-on-insulator
RIE	Reactive Ion Etching
VLS	Vapor-Liquid-Solid
AAM	All Area Modification
SSM	Single Surface Modification
APTM	Aminopropyltrimethoxysilane
PDMS	Polydimethylsiloxane
SEM	Scanning Electron Microscope
GSH	Glutathione
GST	Glutathione S-transferase
EDTA	Ethylenediaminetetraacetic acid
MPTMS	Mercaptopropyltrimethoxysilane
DTT	Dithiothreitol
PSA	Prostrate Specific Antigen
GQD	Graphene Quantum Dot
SS	Subthreshold Swing
GAA	Gate-all-around

Acknowledgements

We would like to thank our thesis supervisor, Dr. Syed Iftekhar Ali, for his continuous guidance and motivation in completing our thesis. His constant inspiration and demand for making the work more comprehensive led us to satisfactory results. We were provided with many useful information and important theories by him to carry out our work with constant diligence as a great outcome.

Abstract

The detection of biological and chemical species is central to many areas of healthcare and the life sciences, ranging from uncovering and diagnosing disease to the discovery and screening of new drug molecules. Hence, the development of new devices that enable direct, sensitive, and rapid analysis of these species could impact humankind in significant ways. Devices based on nanowires are emerging as a powerful and general class of ultrasensitive, electrical sensors for the direct detection of biological and chemical species.

Development of nanobiosensor is one of the most recent advancement in the field of Nanotechnology. Research on optical nanobiosensors with submicron-sized dimensions has opened new horizons for intracellular measurements. Taking advantage of the unique properties of the nanomaterials, faster and sensitive nanobiosensors can be developed. Apart from being sensitive and fast, the studies related to nanobiosensors have geared their efforts towards the development of nanomaterial-based sensors that are affordable, robust and reproducible. The nanobiosensors are equipped with immobilized bioreceptor probes, *e.g.*, antibodies, enzyme substrate. Laser excitation is transmitted to photometric system in the form of optical signal (fluorescence). Nanobiosensors will revolutionize the future of disease diagnosis. The present review discusses the basic concepts, developments and the biomedical applications of nanobiosensors.

Chapter 1

Introduction

Sensing the biological responses has assumed great significance in the current scenario of ever dynamic environmental developments and corresponding altered homeostatic happenings occurring at both *in vivo* as well as *ex vivo* levels. The analysis of behavior of the ever changing materials has assumed great significance in areas like pharmaceutical diagnosis, screening food quality, and environmental applications. In this reference, the development of efficient biosensors which can analyze the minutest details of the biological interactions even at a very small scale and with extreme precision and maximum ever possible sensitivities deserves urgent attention [1].

A key component of the biosensing is the transduction mechanisms which are responsible for converting the responses of bioanalyte interactions in an identifiable and reproducible manner using the conversion of specific biochemical reaction energy into an electrical form. Through the use of transduction mechanisms, nanomaterials can be wonderful incumbents in this dimension as they have high surface area to volume ratios which allow the surface to be used in a better and far more diversely functional manner. Moreover, their electromechanical properties are the wonderful assets for the biosensor technology. Nanostructural wonders provided by nanotechnology have revolutionized the happenings in the domain of molecular biology which have provided an opportunity for manipulation of atoms and molecules and monitored the biological phenomenon at the physiological level with far greater precision. The terminology nanobiosensors a misnomer in the sense that it has the word nano prefixed to it. To get to the real technology, one must soundly gather the idea of what a biosensor is. As nanoscience is interdisciplinary in nature so putting the word nano as prefix often implies the use or manipulation at a scale equivalent to one-billionth of a meter.

1.1 What is Biosensor

A biosensor can be defined as a sensing device or a measurement system designed specifically for estimation of a material by using the biological interactions and then assessing these interactions into a readable form with the help of a transduction and electromechanical

interpretation. In terms of the conceptual and fundamental mode of operation, these components are, namely, bioreceptor, transducer, and the detector.

The main function or purpose of a biosensor is to sense a biologically specific material. Often, these materials are antibodies, proteins, enzymes, immunological molecules, and so on. It is done by using another biologically sensitive material that takes part in the making of bioreceptor. So, a bioreceptor is that component of a biosensor which serves as a template for the material to be detected. There can be several materials which can be used as bioreceptors. For instance, an antibody is screened using antigen and vice versa; a protein is screened using its corresponding selective substrate and so on.

The second component is the transducer system. The main function of this device is to convert the interaction of bioanalyte and its corresponding bioreceptor into an electrical form. The name itself defines the word as ‘trans’ means change and ‘ducer’ means energy. So, transducer basically converts one form of energy into another. The first form is biochemical in nature as it is generated by the specific interaction between the bioanalyte and bioreceptor while the second form is usually electrical in nature. This conversion of biochemical response into electrical signal is achieved through transducer.

The third component is the detector system. This receives the electrical signal from the transducer component and amplifies it suitably so that the corresponding response can be read and studied properly. In addition to these components, a very essential requirement of the nanobiosensors is the availability of immobilization schemes which can be used to immobilize the bioreceptor so as to make its reaction with bioanalyte much more feasible and efficient. Immobilization makes the overall process of biological sensing cheaper, and the performance of the systems based on this technology is also affected by changes in temperature, pH, interference by contaminants, and other physicochemical variations [2].

1.2 Fusion of Nanotechnology and Biosensors: Nano-biosensors

Nanobiosensors are basically the sensors which are made up of nanomaterials and interestingly these are not the specialized sensors which can detect the nanoscale events and happenings. Nanomaterials are a unique gift of nanotechnology to the mankind; these are the materials which have one of their dimensions between 1 and 100 nanometers. The size

constraints of these materials makes them very special as they have most of their constituent atoms located at or near their surface and have all vital physicochemical properties highly different from the same materials at the bulk scale.

They can play very efficient roles in the sensing mechanism of the biosensor technology. Integrated devices of the nanomaterials with electrical systems give rise to nano-electro-mechanical systems (NEMS), which are very active in their electrical transduction mechanisms.

Several nanomaterials have been explored on the basis of their electronic and mechanical properties for their use in improved biological signaling and transduction mechanisms. Some of such materials that are widely employed include nanotubes, nanowires, nanorods, nanoparticles, and thin films made up of nanocrystalline matter [3]. Amongst these, the use of nanoparticles is best studied and analyzed till date. These can be as diverse as using amperometric devices for enzymatic detection of glucose to using quantum dots as fluorescence agents for the detection of binding and even using bio conjugated nanomaterials for specific biomolecular detection. These include colloidal nanoparticles which can be used to conjugate with antibodies for immunosensing and immunolabelling applications.

These materials can also be used to enhance the electron microscopic detections. Further, metal based nanoparticles are very excellent materials for electronic and optical applications and can be efficiently used for detection of nucleic acid sequences through the exploitation of their optoelectronic properties.

1.3 Different Types of Biosensors

1.3.1 Nanoparticle Based Sensors

- ***Acoustic Wave Biosensors***

Acoustic wave biosensors have been developed to amplify the sensing responses so as to improve the overall preciseness of the limits of biodetection. There can be so many stimulus based effects in these kinds of sensors. The mass based variant of these sensors involves the conjugation of antibody modified sol particles which bind themselves on the electrode surface that has been complexed with the particles of analyte conjugated in a manner that antibody

molecules are immobilized over the electrode surface. The large mass of bound sol particles of the antibody results in a change in the vibrational frequency of the quartz based sensing platform, and this change acts as the basis of detection.

In general, the preferred diameter of the sol based antibody particles is between 5 and 100 nm. Particles of gold, platinum, cadmium sulphide, and titanium dioxide are generally preferred [4, 5].

- ***Magnetic Biosensors***

Magnetic biosensors utilize the specially designed magnetic nanoparticles. These are mostly ferrite based materials, either used individually or in combined form. These types of sensors are very useful with reference to the biomedical applications. The magnetic materials enable a great deal of diversity for several analytical applications. This is so because the magnetic compounds involved in screening constituted of iron coupled with other transition metals, which have different properties. With the incorporation of magnetic nanoparticles, the conventionally used bio 2 detection devices have further become more sensitive and powerful. Alloys of transition metals with iron and other materials having unpaired electrons in their d-orbitals have been highly versatile in their magnetic behaviors. A very popular kind of materials that have come to the fore involving these employs magnetic bioassay techniques that are used for specific isolation of magnetically labeled targets with the help of a magnetometer [6].

Special devices such as superconducting quantum interference devices (SQUID) have been used for rapid detection of biological targets using the super paramagnetic nature of magnetic nanoparticles. These devices are used to screen the specific antigens from the mixtures by using antibodies bound to magnetic nanoparticles [7]. These make use of super paramagnetic effect of magnetic materials which is particularly observed in the nanoscale particles.

- ***Electrochemical Biosensors***

These sensors basically work to facilitate or analyze the biochemical reactions with the help of improved electrical means. These devices are mostly based on metallic nanoparticles. The chemical reactions between the biomolecules can be easily and efficiently carried out with

the help of metallic nanoparticles, which significantly help in achieving immobilization of one of the reactants. This ability makes these reactions very specific and eliminates any possibility of getting undesirable side products. In this reference, colloidal gold based nanoparticles have been used to enhance the immobilization of DNA on gold electrodes which has significantly increased the efficiency of an overall biosensor by further lowering the detection limit [8]. Biosensors have been designed using enzyme conjugated gold nanoparticles for the identification of glucose, xanthine, and hydrogen peroxide [9-11].

In a significant study by Xu et al., the analysis of electrochemistry of enzyme systems comprising of horse reddish peroxidase, on gold electrodes loaded with nanoparticles of carbon, has been put forward [11]. The study predicted a faster amperometric response and faster and much better electrocatalytic reduction ability for horse reddish peroxidase. As a result, the biosensor developed showed improved sensitivity and much lower detection limit as compared to the one without using nanoparticles.

In a similar trend, nanosized semiconductor crystals can be used to improve the efficiency of photochemical reactions and can be tagged to biological entities like those of enzymes and precursors to design novel photo electrochemical systems. In this dimension, Curri et al. (2002) have used immobilized nanocrystalline CdS using self-assembly approach so as to prepare an enzymatic detection system based on immobilized formaldehyde dehydrogenase onto the gold electrodes in order to carry out the catalytic oxidation of formaldehyde [12].

In several other studies, metal based nanoparticles have been used for coupling themselves with biological probes and then carry out useful detection of the specific molecules from a mixture. Bioassays based on biotin streptavidin specificity have been designed in this regard [13].

1.3.2 Nanotube Based Sensors

Carbon nanotubes are one of the most popular nanomaterials known right now in the world of material science and optoelectronic applications. Since their discovery in 1990's, they have attracted interest worldwide because of their extraordinary properties, the most vital of which are the electronic conductivity, flexible physical geometric features, and the ever

dynamic physicomechanical properties ranging from high aspect ratios to very good functionalization abilities along with having high mechanical strength and folding abilities. Because of these attributes, both single walled nanotubes as well as multi walled nanotubes have been used in designing biosensors for better and better performances [14, 15].

The most popular sensing advances that have come to the fore are the developments in the design of glucose biosensors that involve the use of nanotubes as immobilizing surfaces for enzyme glucose oxidaze; this enzyme is used for estimation of glucose from the several body fluids. In convention, the sensors using enzymes predicted the presence of glucose from major body tissues but the use of nanotubes as assemblies for immobilization has led to the estimation of glucose from even scarce body fluids such as tears and even saliva.

In one such arrangement, single walled nanotubes have been wonderfully employed for enzymatic detection of glucose, and this innovation has also yielded significant increase in the enzyme activity [16]. The enhanced performance of the biosensor was analyzed and found so, largely due to the high enzyme loading and better electrical conductivities of the nanotubes. Not only with their structural flexibilities, carbon nanotubes have also been used for enhancing the electrical detection of the sensing phenomenon, owing to their better and smoother electron transfer flow characteristics. The significant improvements in the catalytic biosensors have been widely exploited in several studies, and in one such study, this innovation resulted in better oxidoreductase performance in both glucose oxidase and flavin adenine dinucleotide precursors binding to their substrates more efficiently and in a much more controllable manner [17].

Likewise, chemoelectroluminiscence effect has been improved by coupling CNTs to the sensing molecules of a sensor through better conductance of charge carriers and controlling their required flow characteristics. In a significant and comprehensive review, biosensors based on carbon nanotubes have been extensively summarized for key breakthroughs and advantages that they get bestowed with, by the incorporation of nanostructured arrays of carbon nanotubes and the related structure sensitive assemblies. This review highlights the functionalization potential of carbon nanotubes and their rapid friendliness for being coupled with biomolecules like DNA, proteins, oligonucleotide probes and their corresponding benefits in an excellent manner [18].

1.3.3 Nanowire Based Sensors

Nanowires are cylindrical arrangements just like those of carbon nanotubes, having lengths in the order of few micrometers to centimeters and diameters within the nano range. Nanowires are the one dimensional nanostructures with very good electron transport properties. Significantly, the motion of charge carriers in the nanowires is vigorously improved and different from those in bulk materials. Sensors based on nanowires are very less in number, but literature reports some exciting examples where use of nanowires has significantly improved the performance and detection of biological materials.

In one such study, Cui and Lieber group have reported the performance of biosensors based on silicon nanowires doped with boron and used them for the detection of biological and chemical species [19]. Semiconductor nanowires have been exploited in a great detail and have also been used for coupling a number of biomolecules for identifying their specifically linked substrates.

In a study, silicon nanowires coated with biotin have been used for the detection and isolation of streptavidin molecules from a mixture. The small size and capability of these nanowires make them ideal candidates to be used for biodetection of pathogens and many other real time analysis of a wide range of biological and chemical species, thus vastly improvising the current accuracies of presently used *in vivo* diagnostic procedures. As these sensing materials work on very precisely defined dimensions, they can also be used to accomplish *in vivo* applications and operate in the smallest environments within the living cells.

In one such study, Wang et al. have used optical fibers with diameters in the nanosize and coated with antibodies to detect the presence of toxicants within the single cells [20]. In another very closely related study, Cullum et al. have reported the synthesis of ZnO nanowires, coated them over the gold electrodes, and then used them for detection of hydrazine using amperometric responses [21]. They have proposed a high sensitivity, low detection limit, and far lower response times than those reported in the conventionally used reported in the conventionally used sensor systems.

Nanowires are very versatile in their performance and are significantly better than nanotubes in two major ways. First, they allow a range of modifications in their design by

control of operational parameters during their synthesis. Secondly, they possess a lot much more scope for the development of functionalized assemblies by virtue of the existence of compatible materials on their surfaces.

Despite very well-known synthesis procedure for nanowire synthesis, their use in the development of sensing devices has met several challenges [22]. It has been reported by several related studies that it is difficult to incorporate nanowires into the sensing systems for the overall improvement in their electrical conductivities to be realized. In a very advanced study, Lieber group have rigorously worked on semiconductor nanowires and synthesized them by using combinations of previously known methods. They have developed a complex one dimensional architecture comprising of at least 200 independent electrical nanowire assemblies and have used them to perform a low level detection of serum-bone cancer antigens [19].

For the best analysis of rationale behind using nanowires or knowing about their qualities that can improve sensing mechanism, Yang et al. provided a valuable insight by rigorously talking about nanowires and nanobelts as well as their structural aspects and features through which they can be used in sensing applications [23]. In a couple of related advancements, both Cui et al. and Huang et al. have explored the salient attributes of nanowires and explained their utility in better conduction and detection of biological stimulus [24,25]. Huang et al. have particularly focused on surface plasmon resonance ability of nanowires, through which these can be incorporated into the sensing probes and significantly improve the sensitivity of sensing event.

To make the process little more simplified, Stern et al. have developed nanowires through the complementary metal oxide semiconductor (CMOS) approach. This approach has proved to be very easy in terms of controlling and regulating the synthesis procedures for nanowires and has been used for analysis of serum fluids so as to enable the isolation of several pathogens and proteins in crude form [26]. In this way, nanomaterials have proved to be highly prosperous for brightening the sensing technology and have improved the diagnostic and detection procedures by leaps and bounds. The faster and quicker diagnosis enabled by still faster analysis and evaluation protocols through the nanomaterials has just revolutionized the biosensing mechanism.

There are many other nanomaterials except those mentioned above that have been capitalized upon and made use of in biosensing applications. Nanodots resembling the morphology of quantum dots, nanosheets, and many other structures of altered geometries such as nanocombs, nanobelts and nanoribbons have been used for improving the conventional procedures of sensing. The coupling of piezoelectric and cantilever systems has further added a new charm to this technology. Nanomaterials like quantum dots have been added as labels coupled with sensitive dyes, and they have yielded thermochromic, photochromic, and electro chromic materials which can show highly sensitive detections that can be monitored easily. They have significantly helped in improving electron transport mechanisms and also in the development of much more efficient actuating mechanisms to impose a particular state of observation on a system. The text ahead mentions some impact provoking applications of nanobiosensors in the different walks of life.

Chapter 2

Operation and Fabrication of Nanowire Biosensors

2.1 Working Principles of Nano-biosensors

A common FET nano-biosensor includes the structure of a three-electrode transistor. The drain and source electrodes are connected by the semiconductor channel as well as the gate electrode modulates conductance of the channel [27]. The structure of an FET sensor is illustrated in (Fig. 1).

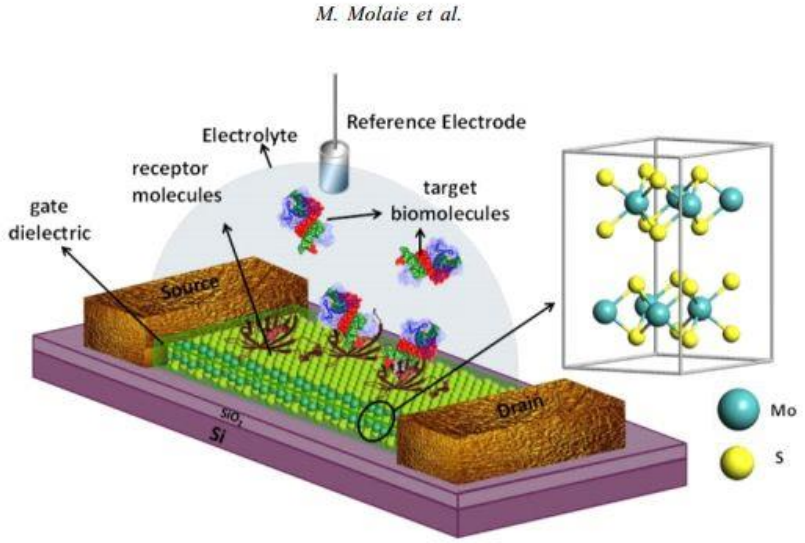

Fig. 1. Typical 2D MoS2-based FET biosensor device. For biosensing, the dielectric layer covering the MoS2 channel is functionalized with receptors for specifically capturing the target biomolecules. The thickness of the MoS2 flake used is 5 nm. Reprinted and/or adapted with permission from [17] (Copyright © 2014, American Chemical Society).

Channel as a "sensing" component of the FET nanosensor device is made of 1D or 2D nanomaterials [28]. In order to identify a unique analyte via FET nanosensors, a specific recognition group which is also called a probe, ligand, or receptor is employed. This recognition group is anchored to the surface of the semiconductor channel. It's clear that for providing a high degree of both specificity and affinity in FET biosensors, each specific receptor should be employed to realize its target analyte.

Then, according to the type of receptor used for the target molecule diagnosis, FET biosensors can be classified into several groups such as DNA-modified FETs, immunologically

modified FETs, enzyme-modified FETs and cell-based FETs. The semiconductor used as a channel has a consistent conductance and is specified by main carrier density in the nanomaterials which can be determined from the source-drain current in device, so carrier density is proportional to the conductance of the channel (electrons for an n-type semiconductor or holes for a p-type semiconductor).

Therefore any change in the conductance of the channel change generates change in the source-drain current. An electric field is generated on the surface when a charged molecule (analyte) binds to a receptor anchored on the nanomaterial, and this connection exerts an effect outside and inside of the channel [29].

For instance, when an analyte molecule such as DNA with a negative charge binds to the p-type channel, due to the charge of analyte is opposite to the main carriers in the channel, the charge carriers will accumulate under the bound analyte, which causes a buildup of hole carriers and consequently an increase in conductivity of device will be displayed. This mechanism is shown in Route A in (Fig. 2).

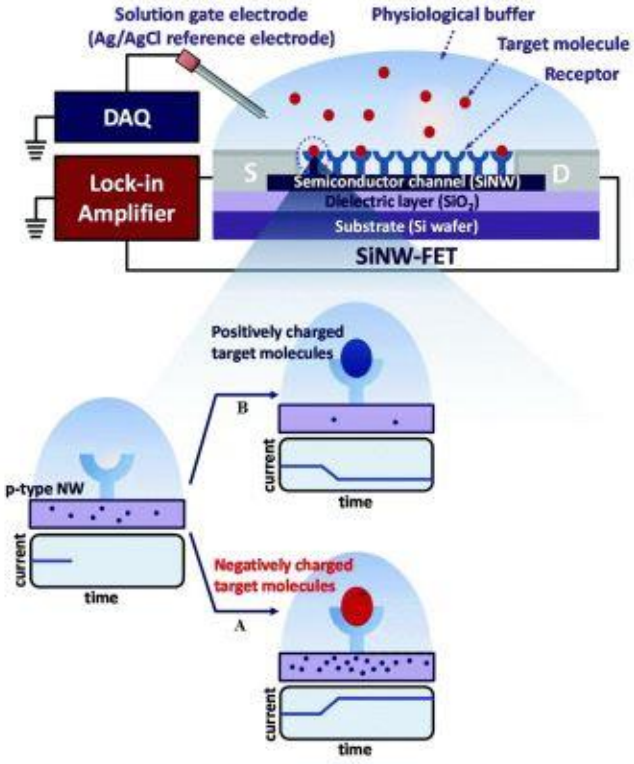

Fig. 2. Mechanism to modulate the conductance of a p-type nanomaterial-based FET (holes as the main charge carriers). Reprinted and/or adapted with permission from [12] (Copyright © 2013, Royal Society of Chemistry)

On the other hand if a positively charged molecule, such as a protein binds to the p-type channel, a depletion of main carriers beneath the bound analyte in the device channel and a decrease in conductivity will occur. This case is illustrated in Route B in (Fig. 2). The source-drain current of the channel is monitored against time. In route A, when a negatively charged target binds to the receptor anchored on the nanomaterial, the charge carriers will accumulate under the bound analyte that causes an increase in the device conductivity and source-drain current. In route B, the binding of a positively charged target leads to depletion of charge carriers beneath of the bound analyte, causes a decrease in conductivity and source drain current [27]. The mechanism of the conduction changing during molecular binding is also a debated topic [31-34]. According to the ideal transistor linear (region often used for biosensing) current equation is:

$$I_{ds} = \mu C_{ox} \frac{W}{L} [(V_{GS} - V_T)V_{ds} - \frac{1}{2} {V_{ds}}^2]$$

$$V_T = E_{ref} - \psi - \chi^{sol} - \frac{\emptyset_{si}}{q} - \frac{Q_t}{C_{ox}} + 2\emptyset_f$$

Where μ = channel mobility,

C_{ox} = dielectric capacitance,

W = width of the device

L = length of the device,

V_T = threshold voltage of the device,

A surface potential (ψ) develops at the dielectric-solution interface,

χ^{sol} = surface dipole potential of the solvent,

$\emptyset_{si}$ = the channel work function,

q = elementary charge,

Q_t = combination of depletion charges in the semiconductor, accumulated charges in the dielectric, and interface trap charges, and

$\emptyset_f$ = Fermi potential.

The only variable term in the equation is $\boldsymbol{\psi}$, which is a function of physical and chemical changes at the surface of the oxide. Thus, monitoring changes via the change in V_T is an effective way of sensing changes at the dielectric electrolyte interface. While the transistor dimensions (A, d, and L) and the drain voltage (V_{ds}) are constant, a change in conduction current (I_{ds}) can be caused by either a change in mobility (μ), a change in capacitance due to

the difference in the dielectric constant (ε_r) of the sensing environment versus the binding molecule, or a gating effect (V_{GS}) caused by charges from the binding molecule.

2.2 Fabrication of Nanowire FETs

There are two major fabrication techniques in preparing SiNW-FETs: ‘‘top-down’’ and ‘‘bottom-up’’. The ‘‘top-down’’ method is carried out through lithographic processes combined with an electron-beam technique that defines SiNW-FETs by physically etching a single-crystalline silicon wafer [39]. On the other hand, the ‘‘bottom-up’’ processes start with the growth of SiNWs, normally in a chemical vapor deposition (CVD) reaction, followed by SiNW assembly and electrode fabrication via the photolithographic or electron beam lithographic procedures [36].

2.2.1 ‘Top-down’ SiNW-FETs

The ‘‘top-down’’ method for the SiNW-FET fabrication is based on lithographic processing on a silicon-on-insulator (SOI) wafer. As illustrated in Fig. 3(a, i), the structure of an SOI wafer contains three layers: substrate Si wafer, buried silicon dioxide (about 200—400 nm thick), and top Si layer (about 50—100 nm thick). Through the standard procedures of photolithography, reactive ion etching (RIE), ion implantation, electron-beam lithography, and thermal evaporation, SiNWs and the connecting electrodes can be defined to form SiNW-FET devices, in which the width of SiNWs could reach the scale of ~100 nm.

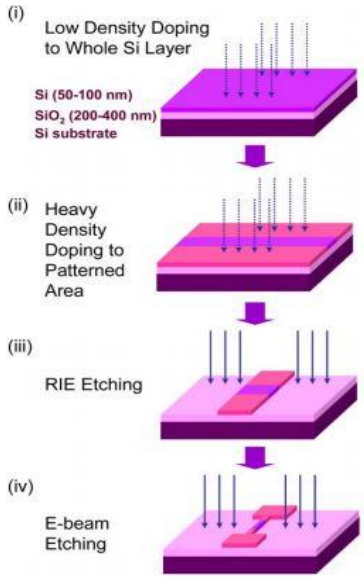

Figure 3 (a) Schematic illustration of a typical ‘‘top-down’’ process to fabricate SiNW-FETs. (i) In Step 1, the silicon layer is doped with low-density boron or phosphorous of $\sim 10^{15}/cm^3$. (ii) In Step 2, specific regions defined with a photomask pattern receive heavy doping ($10^{19}/cm^3$). (iii) In Step 3, the micrometer-sized source and drain electrodes are finished by RIE etching. (iv) The following Step 4 is to fabricate the nanometer-sized SiNWs with an electric-resist pattern and RIE etching.

A typical ‘‘top-down’’ process to fabricate SiNW-FETs is illustrated schematically in Fig. 3(a) [47—54].

- In Step 1, the Si layer is doped with low-density boron or phosphorous of $\sim 10^{15}/cm^3$ (about 10—20 cm). Therefore, the n/p type semiconducting property and doping ratio of SiNWs are determined (Fig. 3(a, i)).
- Step 2 is to define the source and drain leads with heavy doping ($10^{19}/cm^3$), of which the patterns are drawn with a photomask design (Fig. 3(a, ii)).
- In Step 3, the micrometer-sized source and drain electrodes are finished by RIE etching (Fig. 3(a, iii)).
- The following Step 4 is to fabricate the nanometer-sized SiNWs with an electric-resist pattern and RIE etching (Fig. 3(a, IV)).

Subsequently, a thermal evaporation is used to make the contact leads and back-gate, and finally an insulator layer (e.g., Al_2O_3 [40, 44], SiO_2 [42], or Si_3N_4 [47]) is coated on the SiNW-FET devices. Compared with the ‘‘bottom-up’’ method, the ‘‘top-down’’ approach is more complex because the process relies on high-resolution lithography. For this reason, electron-beam lithography is necessary. Although the ‘‘top-down’’ approach needs many luxurious instruments, it has advantages of using standard semiconductor techniques to precisely design a desired device-array pattern without problems of positioning SiNWs. Another challenge to the ‘‘top-down’’ method is that the minimum width of the produced SiNWs is around 100 nm. To overcome this barrier, single SiNWs of triangular section were fabricated to reach the transverse dimension of ≤20 nm with the length of several micrometers [46].

2.2.2 ‘Bottom-up’ SiNW-FETs

The ‘‘bottom-up’’ processes start with the growth of SiNWs, normally in a chemical vapor deposition (CVD) reaction, followed by SiNW assembly (assisted by various techniques that

are discussed in the next section), and finally the device fabrication via the photolithographic or electron beam lithographic procedures [36].

- With the ‘‘bottom-up’’ method, SiNWs can be synthesized catalytically in a CVD reaction via the vapor—liquid—solid (VLS) growing mechanism (Fig. 3(b, i)) [48].
- The synthesis is usually catalytically assisted with metal nanoparticles [49, 50] that not only catalyze the SiNW formation, but also control the size of the as-synthesized SiNWs. Subsequently, the as-synthesized SiNWs are suspended in ethanol solution and dispersed onto a support silicon substrate (Fig. 3(b, ii)).
- In the following photolithographic steps, a two-layer photoresist consisting of LOR3A and S1805 was first deposited onto a silicon substrate by spin coating where the electrodes were defined with a photomask design (Fig. 3(b, iii)).
- The next step is 136 K.-I. Chen et al. to deposit metal for the source/drain contacts by thermal evaporation (Fig. 3(b, IV)). Finally, the remaining photoresist layer was lifted off by Remover PG (Fig. 3(b, v)) [36].

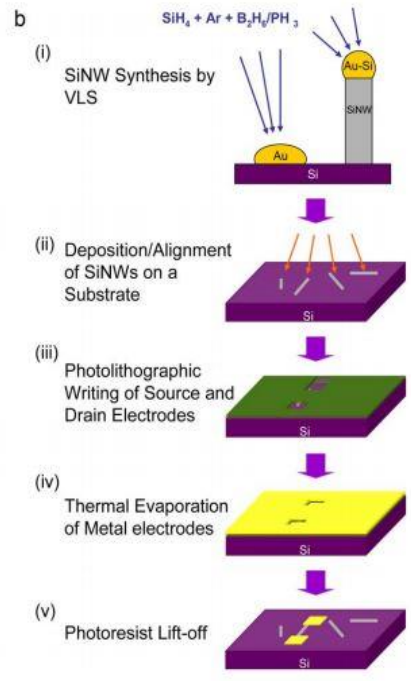

Fig. 3 (b) an illustration of a ‘‘bottom-up’’ method to fabricate SiNW-FETs. (i) The growth of SiNWs in CVD reaction via the VLS mechanism. (ii) Deposition/alignment of SiNWs on a silicon substrate. (iii) A photomask pattern to define source/drain electrodes. (iv) Thermal evaporation to deposit the source/drain contacts. (v) Lift-off the remaining photoresist with Remover PG.

Compared with the ‘‘top-down’’ technique, the ‘‘bottom-up’’ method has the advantages of synthesizing SiNWs of high crystallinity, designated dopant density, thin silicon oxide sheaths, and easily controlled diameters in a cost-effective preparation. However, without a deliberate alignment for the randomly orientated SiNWs on the silicon substrate, the device fabrication would suffer from inefficient fabrication yields, which could also limit their development in the industrial applications. Therefore, the success of producing high-quality SiNW-FETs calls for developing a uniform assembly of the ‘‘bottom-up’’ synthesized SiNWs on the support substrates.

In recent years, 1D FETs using polymeric nanowires including deuterated polymer (DP), polyaniline (PANI), polycarbonate (PC), polyvinyl alcohol (PVA), polyvinylpyrrolidone (PVP), polystyrene (PS), polymethyl methacry-late (PMMA) and polyacrylamide (PAM) have been developed. In compare to the physical or chemical nanolithography techniques used for semiconductor wires, fabrication of polymeric nanowires through one-step drawing technology and electro spinning method provide more customizable functionalization and cheaper fabrication that can be widely applied and promoted, but polymeric nanowires show inferior electrical characteristics [52-55].

While the bottom-up fabrication methods for 1D structures encounter severe integrality issues [56, 57] the top-down methods face slow production rate and high cost [57] so its forming limitation in the usability of these structures. On the other hand, the materials with 2D structure such as CNT, MoS_2 and graphene, due to their atomically thin structures can provide excellent electrostatics and also because of possess planar nature they are suitable to large-scale fabrication and integrated device processing [56, 58]. The micromechanical exfoliation technique has been used to obtain MoS_2 flakes (Fig. 4(a)), Graphene sheets (Fig. 4(c)) and various 2D materials [59]. Nanobiosensors with good performance should possess the following qualities, especially if these devices are being used for bioanalytical applications:

1. Outstanding selectivity or specificity
2. High sensitivity and reproducibility of results
3. Short settling time (time necessity to capture the analyte)
4. Fast recovering time (time to regenerate a device after a measurement)

These qualities are affected by several followed parameters, which are related to fabrication techniques and experimental conditions:

1. Channel nanomaterial dimensions
2. Device geometries
3. Surface modification techniques
4. Delivery system
5. Active measurement parameters
6. Gating the device

2.3 Surface Modification

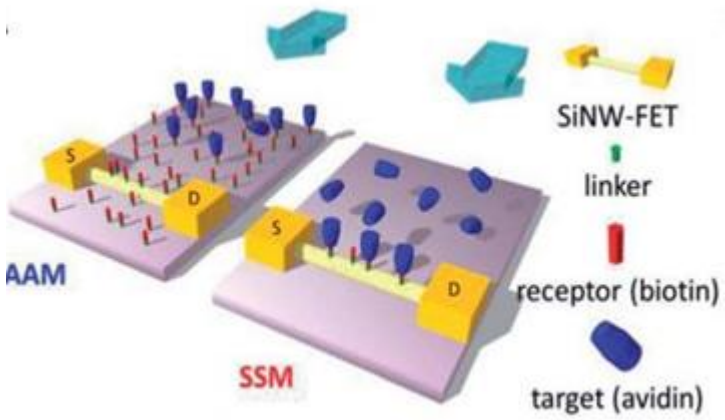

Fig: 4 Surface Modification

2.3.1 AAM Method

- One economical, efficient and commonly used SiNW-FET surface-modification method.
- 3-aminopropyltrimethoxysilane (APTMS), which immobilizes the receptor molecule and anchors to the silica sheath of the SiNW at opposite ends of the linker.
- As the silica sheath on the SiNW surface is no different from the oxidized layer of a Si wafer, receptor molecules are immobilized over the entire silica surface.

The ratio of the surface areas of the SiNW and the surrounding substrate is very small thus large proportion of captured molecules consequently jeopardizes the detection sensitivity such SiNW-FET.

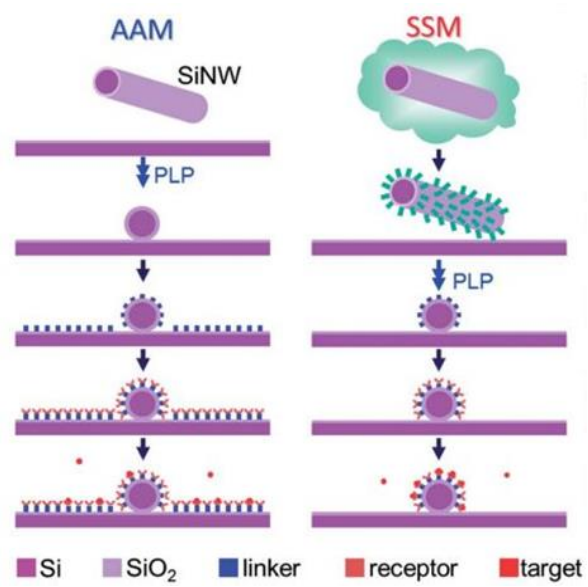

Fig 5: AAM and SSM Methods

2.3.2 SSM Method

Several methods are used here like photolithography, microcontact printing, electrostatic attraction for top-down approach. Recently a bottom up technique has been developed. It is described below:

- In their approach, the SiNWs were modified with APTMS before photolithographic fabrication of the device.

The APTMS molecules modifying the SiNWs survived the harsh photolithographic processes, including photoresist coating, organic solvent washing, and thermal annealing.

2.4 Nanowire Assembly Techniques

Significant efforts have been invested in developing generic methods to align NWs for the device assembly to fabricate NW-FETs. Several techniques for the assembly of NWs have been achieved, including flow-assisted alignment [60], Langmuir—Blodgett technique [61—64], bubble-blown technique [65], electric-field-directed assembly [66—69], smearing-

transfer method [70], roll-to-roll printing assembly [71], and polydimethylsiloxane (PDMS) transfer method [72,73].

Flow-assisted alignment. In the flow-assisted alignment method (Table 1(a)), the suspended SiNWs were passed through the microfluidic channel structures formed between a PDMS mold and a flat SiO_2/Si substrate [60]. The SiO_2/Si substrate was pre-modified with 3-aminopropyltriethoxysilane (APTES), of which one end is anchored to the SiO2 surface and the other end forms an NH_2-terminated surface. This NH_2-terminated surface will help the alignment of SiNWs via electrostatic interactions. While the angular spread of the SiNWs in the flow direction is flow-rate dependent, the density of the SiNWs assembled on the SiO_2/Si substrate is time dependent.

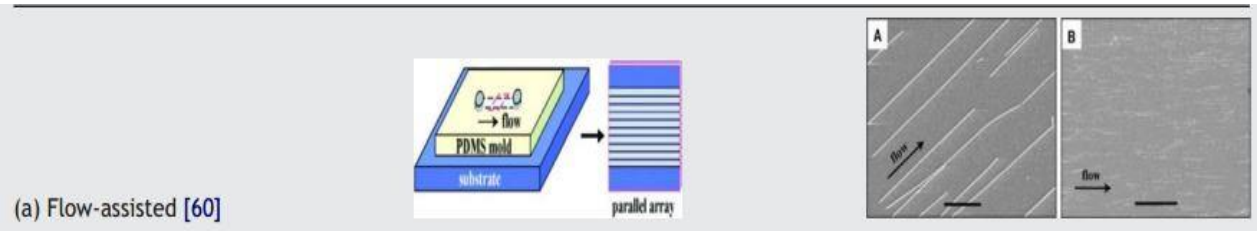

(a) Flow-assisted [60]

Langmuir—Blodgett technique. The Langmuir—Blodgett technique can be applied for the alignment of NWs/NTs. As shown in Table 1(b), this solution-based method assembles SiNWs in a monolayer of surfactant at the air—water interface and then compresses the SiNWs on a Langmuir—Blodgett trough to a specified pitch. The aligned SiNWs are then transferred to the surface of a substrate to make a uniform parallel array. Crossed SiNW structures could further be formed by uniform transfer of a second layer of aligned parallel SiNWs perpendicular to the first layer [61—64]. Compared with other methods, the Langmuir—Blodgett technique can prepare an ultrahigh-density SiNW alignment.

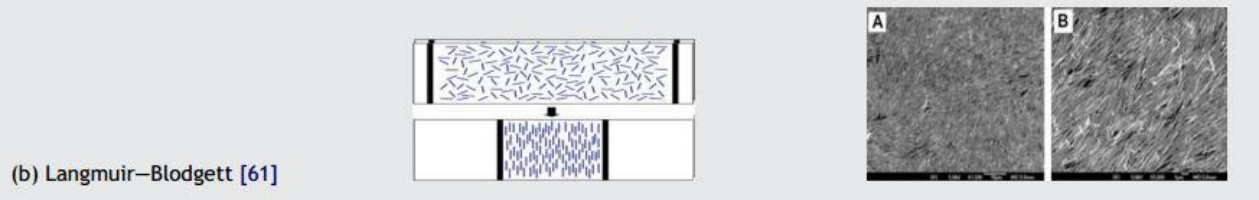

(b) Langmuir–Blodgett [61]

Bubble-blown technique. The bubble-blown technique is another physical assembly method (Table 1(c)), in which the SiNWs were suspended in tetrahydrofuran solution and then blown into a single bubble using a nitrogen flow to form SiNW blown-bubble films [65]. The uniqueness of this method is that blown-bubble films can be transferred to both rigid and

flexible substrates during the expansion process. It can also be scaled to large wafers and non-rigid substrates [65].

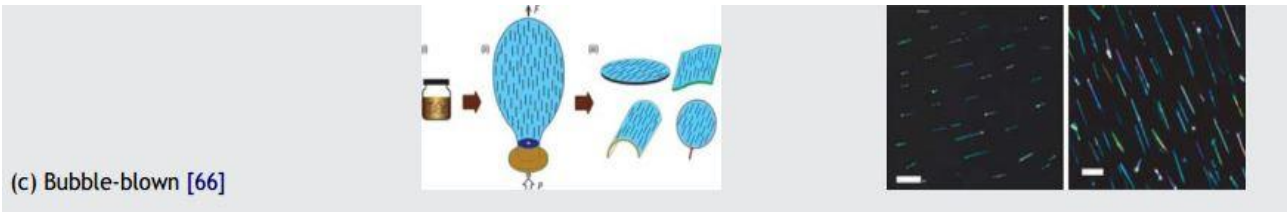
(c) Bubble-blown [66]

Electric-field-directed assembly. The electric-field directed assembly of SiNWs is an intriguing and desirable method. From the appropriate electrode design and adjustment of the applied gate voltage (*V*g) vs. source-drain voltage (*V*sd), Freer et al. reported that single SiNWs could be assembled over 98.5% of 16,000 pre-patterned electrode sites through controlling the balance of surface, hydrodynamic, and dielectrophoretic forces (Table 1(d)) [66].

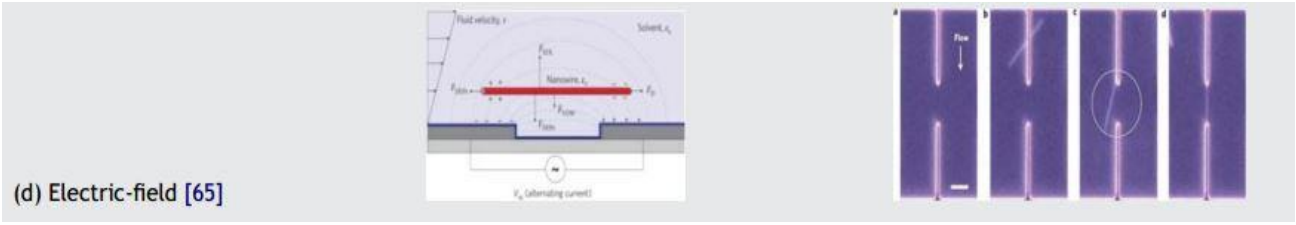
(d) Electric-field [65]

Smearing-transfer method. The smearing-transfer (or contact-printing) method is one of a series of alignment methods developed by Ali Javey's group. This method is based on a direct contact printing process that enables the direct transfer and positioning of SiNWs from a donor substrate to a receiver chip. This simple method can efficiently transfer a variety of NWs (such as SiNWs and Ge-NWs) to a wide range of receiver substrates, including silicon and flexible plastics. The technique actually uses chemical ''lawn'' and ''lubricant'' to increase the density and alignment quality and can be regarded as a rapid, efficient, and economic method (Table 1(e)) [70].

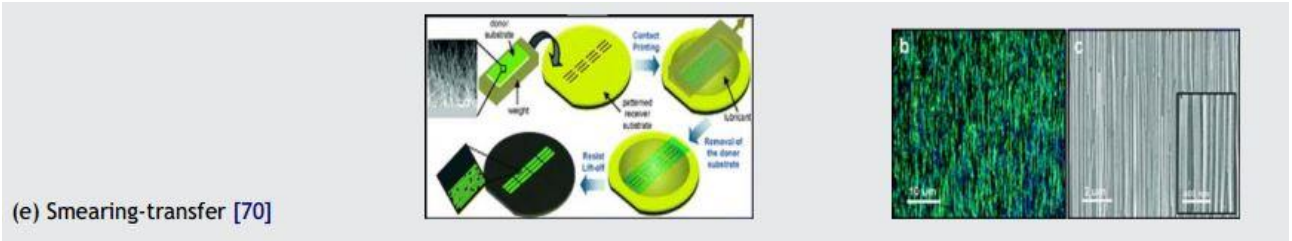
(e) Smearing-transfer [70]

Roll-printing assembly. On the basis of the contact printing process, Ali Javey's group also developed an approach for a scalable and large-area printing. Roll-to-roll assembly has made it possible to produce highly ordered, dense, aligned, and regular arrays of NWs with high uniformity and reproducibility using differential roll printing. The schematic of the differential-roll-printing system setup and the results of the wire alignment are shown in Table 1(f). The optical and scanning electron microscopy (SEM) images of the roller printed Ge-NWs on a Si/SiO_2 substrate clearly indicate the well-aligned and dense (about 6 NWs/m) NW parallel arrays. The differential-roll-printing process is compatible with the smearing-transfer method and can also be implemented in a wide range of rigid and flexible substrates [71].

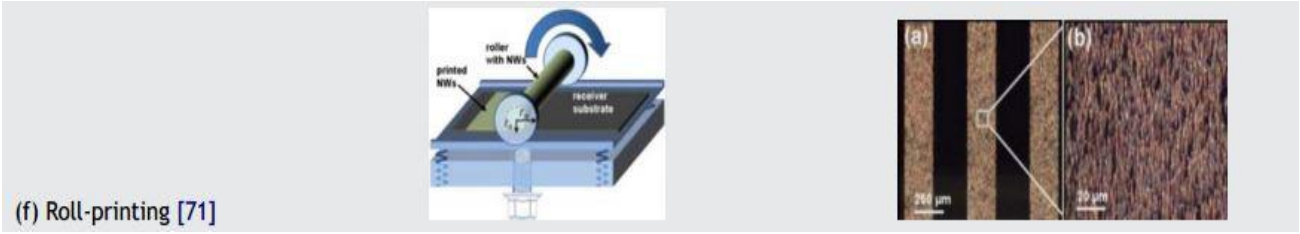

PDMS-transfer method. Chang et al. developed a NW alignment method using a PDMS stamp (Table 1(g)) [72]. In the report, a high-speed roller (20—80 cm/min) was used to assist the transfer of ZnO-NWs from the growth substrate to a PDMS stamp; these NWs were then re-transferred from the PDMS stamp to another receiver substrate. With this method, NWs can be aligned with high density, providing a convenient and efficient approach for the fabrication of NW-FETs.

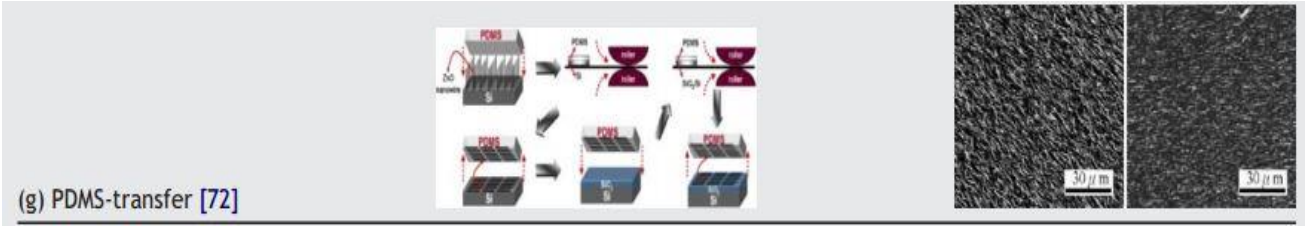

Fig. 6 (a) flow-assisted alignment, (b) Langmuir—Blodgett technique, (c) bubble-blown technique, (d) electric-field-directed assembly, (e) smearing- transfer method, (f) roll-to-roll printing assembly, (g) polydimethylsiloxane (PDMS) transfer method

Chapter 3

Detection of Biomolecules

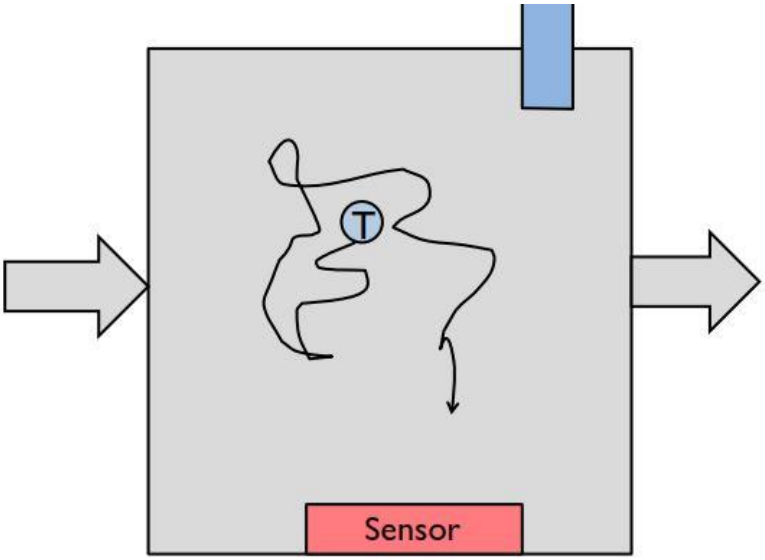

Fig. 7. Biomolecule detection

Let's consider a target molecule T it will diffuse around and ultimately reach the sensor surface. Once it reaches the sensor surface depending on its mass, charge or some other intrinsic physical characteristic the biomolecule would be detected. Now this box could be anything it could be a beaker. It could be a cell wherein a protein molecule is moving around and is getting latched onto another protein.

3.1 Types of Biomolecules

Chemical Indicators: They are small sized biomolecules which causes various diseases:

- Glucose (for diabetes).
- Nitric Oxide (for Parkinson's disease).

Elements of life: They are usually polymers which indicate genetic information or disorders:

- DNA (genetic)
- Protein (Disorders)

Invaders: They are the invaders which come from outside and make us sick they are larger in size:

- Virus (Infection)
- Bacteria (Infection)
- DDT (Disrupts Cell function).

3.2 Properties of Biomolecules

There are several properties of these molecules by the virtue of which we can detect the biomolecules. For electronic biosensing we generally look at:

- Charge
- Redox Potential
- Mass
- Optical Index.

3.3 Size Comparison of different Biomolecules

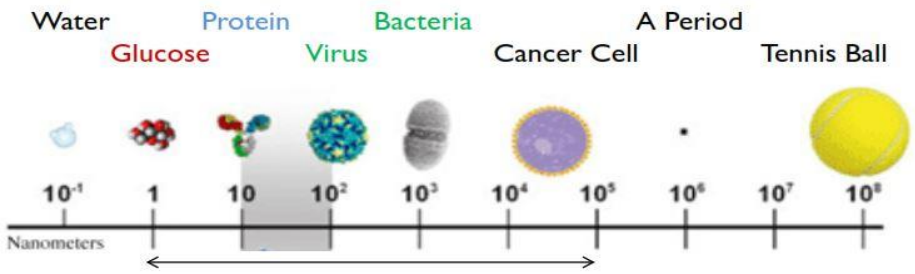

Fig. 8. Size difference of biomolecules

We can easily see the size comparison of the biomolecules. As we go towards the right the size increases. Next we would like to describe particular types of molecules one by one.

Glucose:

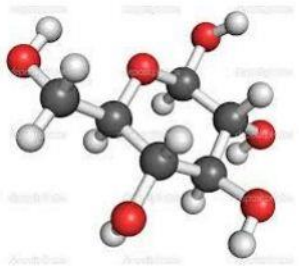

Fig. 9. Glucose

Glucose is a small biomolecule of molecular mass 80g. There is no charge. They are not big and does not have much charge so they are detected by amperometric sensor by electron affinity. The size is approximately 1nm.

DNA:

They are polymers. The diamond shaped are different elements designated A,T,G,C. The hydrogen of the acid makes the molecule negatively or positively charged. The mass is about 300 Dalton.

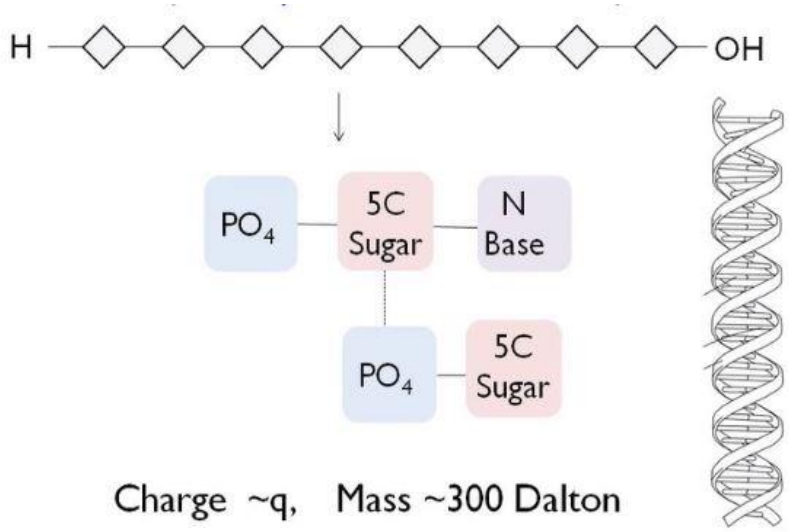

Fig. 10. DNA

Protein:

The protein is biopolymer of charge of variable charge. The mass is about 125 Dalton. They can be Enzymes, Hormones, Tissue, Transport molecules.

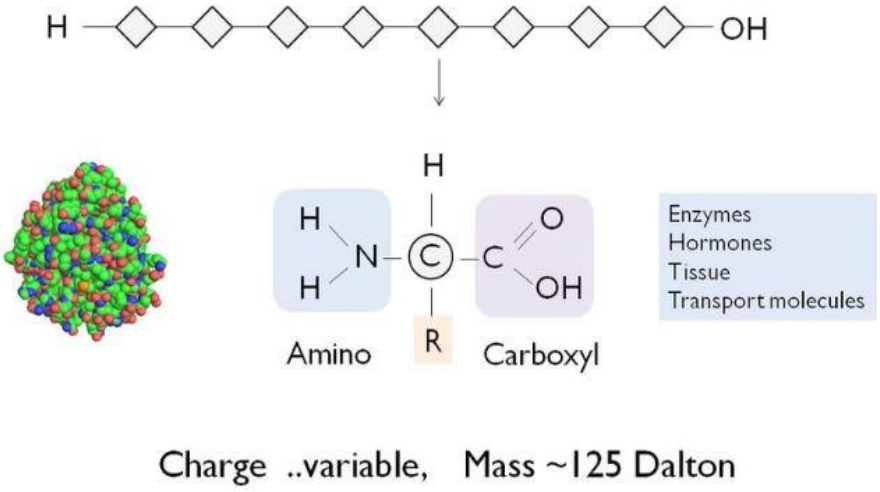

Fig. 11. Protein

There are several protein biomarkers for several disease like:

- PSA for prostrate cancer
- Cardiac TroprinT (CTnT) for heart attack
- Phosphorylation of histone protein (Y-HYAX) for ionizing exposure
- BRCA/ BRCA2 for for breast and overian cancer

Virus:

Fig. 12. Virus

Usually the size is 100 nm and the outer coating is protein where the inside is DNA. Virus doesn't generally carry definite amount of charges, so it is detected by Cantilever sensor. We can have a potentiometric sensor that has a certain amount of pre-existing charge and virus displace some of the charges.

Bacteria:

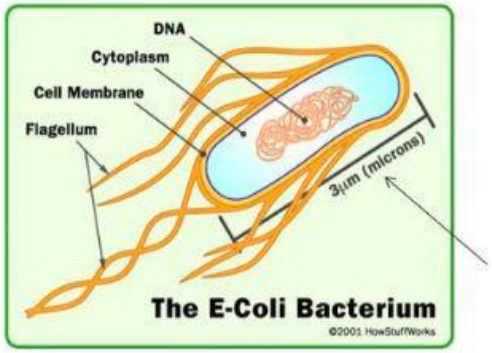

Fig. 13. Bacteria

Bacteria are heavy molecules. 1lb of our weight comes from bacteria. 1mm3 of space may have milllions of bacteria.

3.4 Diffusion of Biomolecules

The biomolecules diffuse around in the analyte randomly. Every molecule in the solution would traverse a different path. They zigzag around because there are invisible water molecule and they collide with them. For a given molecule we cannot say exactly how far it would go in time t. But we can say an average distance each molecule would presumably go. From satistical distribution we get,

$$\frac{d\rho}{dt} = D\nabla^2\rho$$

Where ρ is the concentration of analyte and D is the diffusion coefficient. If we consider total molecules concentrated in a line at time t=0, as the time passes the molecules diffuse away we can derive a equaiton for average distance travelled.

$$\rho(x,t) = \frac{N}{\sqrt{4\pi Dt}} e^{-x^2/4Dt}$$

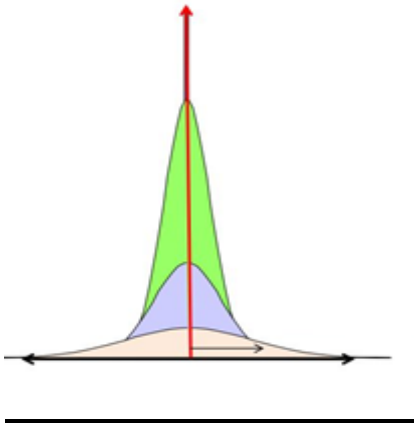

Fig. 14. Diffusion

$$x = \sqrt{Dt}$$

3.5 Some approaches to defeat the diffusion limit

1) Fragmenting Space:

Instead of waiting for a biomolecule to arrive at the sensor surface we can put billions of sensor receptors in the solution looking for the target molecules. The effective box which defines 'L' is reduced. The receptors capture the target and eventually fall on the sensor surface.

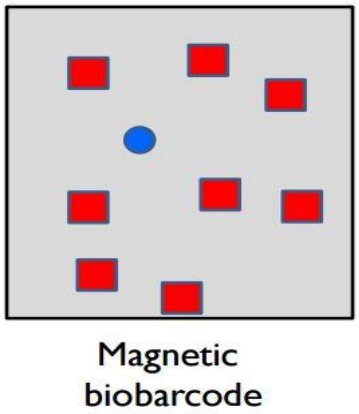

Fig. 15. Biobarcode

2) Droplet evaporation:

Another way to compress the box is to have an analyte droplet and slowly evaporate it. Hence the droplet gradually becomes concentrated and the target molecules comes nearer to the sensor surface.

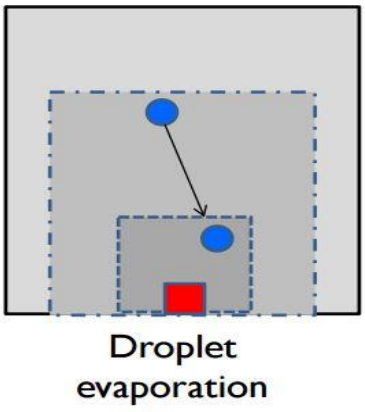

Fig. 16. Evaporation of droplet

3) Generate locally:

Other way to beat the diffusion is to generate very locally. Here the molecules are not coming from a far distance thus L is reduced. Again ‘D’ is high as the molecules are replaced with a smaller cell counterpart.

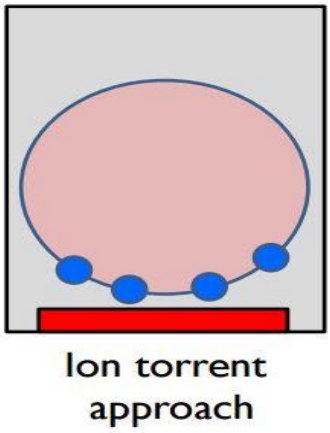

Fig. 17. Generate ion locally

Chapter 4

Sensitivity of Nanowire Biosensors

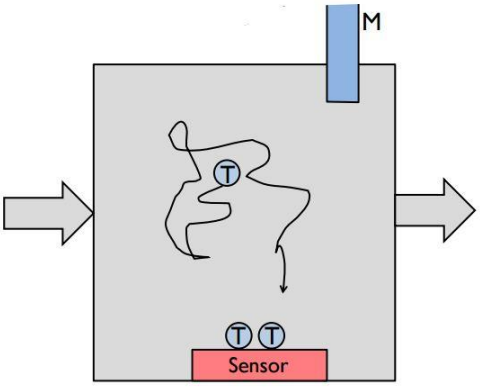

Fig. 6. Biomolecule Detection

4.1 Introducing the sensor

There is a mystery box M which is used as a reference electrode to make the sensor work at noisy environment. After time t the amount of molecules that the surface would catch can be known by a simple differential equation,

$$\frac{dN}{dt} = k_F(N_o - N)\rho_s - k_R N$$

The rate of capture of a molecule is proportional to the no. of probes (receptors) left if all probes are occupied by molecules even if a molecule comes it wouldn't be able to capture that molecule. In the equation K_F is the stickiness coefficient and K_R is the release coefficient. The first part of the equation gives us the capture process where the rate of capture depends on the no. of unoccupied receptors. Now if a molecule is caught and later on it is released due to thermal vibration then second term is important. If we want to look at how many molecules captured we need a balance between capture and release process. The above equation can be analytically solved to get total no. of captured molecules in time t.

$$N(t) = N_{ss}(1 - e^{-(k_F\rho_s + k_R)t})$$

$$N_{ss} = \frac{k_F \rho_s}{k_F \rho_s + k_R} N_o$$

$$k_F \rightarrow \infty, \rho_s \rightarrow \infty$$

Where ρ_s is the steady state concentration and N_{ss} is the steady state capture. N_0 is the initial concentration of the analyte.

4.2 Dependence on geometry

4.2.1 Size effect on sensitivity

- The wire size of a SiNW-FET can also affect the sensitivity of the FET device. The surface-to-volume ratio of thick wires is relatively small compared to that of thin wires.
- Therefore, when thick wires are approached by charged particles, the area affected by the electric field exerted from the charged particles is only located at or close to the wire surface. The interior areas of the wires could still be unaffected.
- In sharp contrast, as the wire diameter decreased, say to nanoscale, the surface-to-volume ratio increases drastically and the influence of the external electric field could reach the whole cross-section of the NW.
- As such, the induced conductance change inside the NW-FET could overwhelmingly prevail over microwire-FETs. Elfstrom et al. have demonstrated the size-dependent sensitivity of Si-NW FETs.

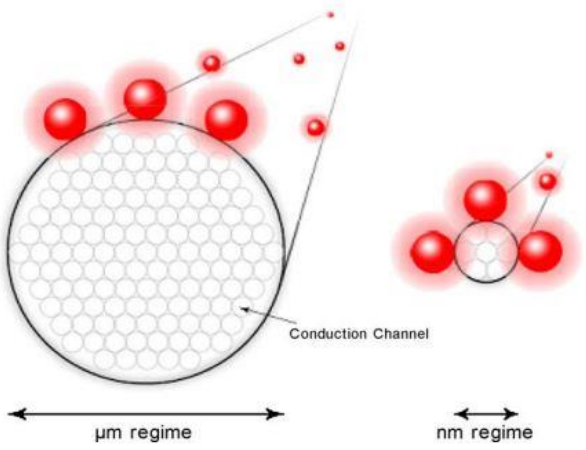

Fig. 18. Size effect on sensitivity

4.2.2 Fractal Dimension

For determining fractal dimension of any surface we repeatedly divide the surface horizontally and vertically and keep a note of the cells occupied. Then plotting a simple logarithmic plot of cells occupied vs the no. of divisions is done. We denote fractal dimension by slope D_F.

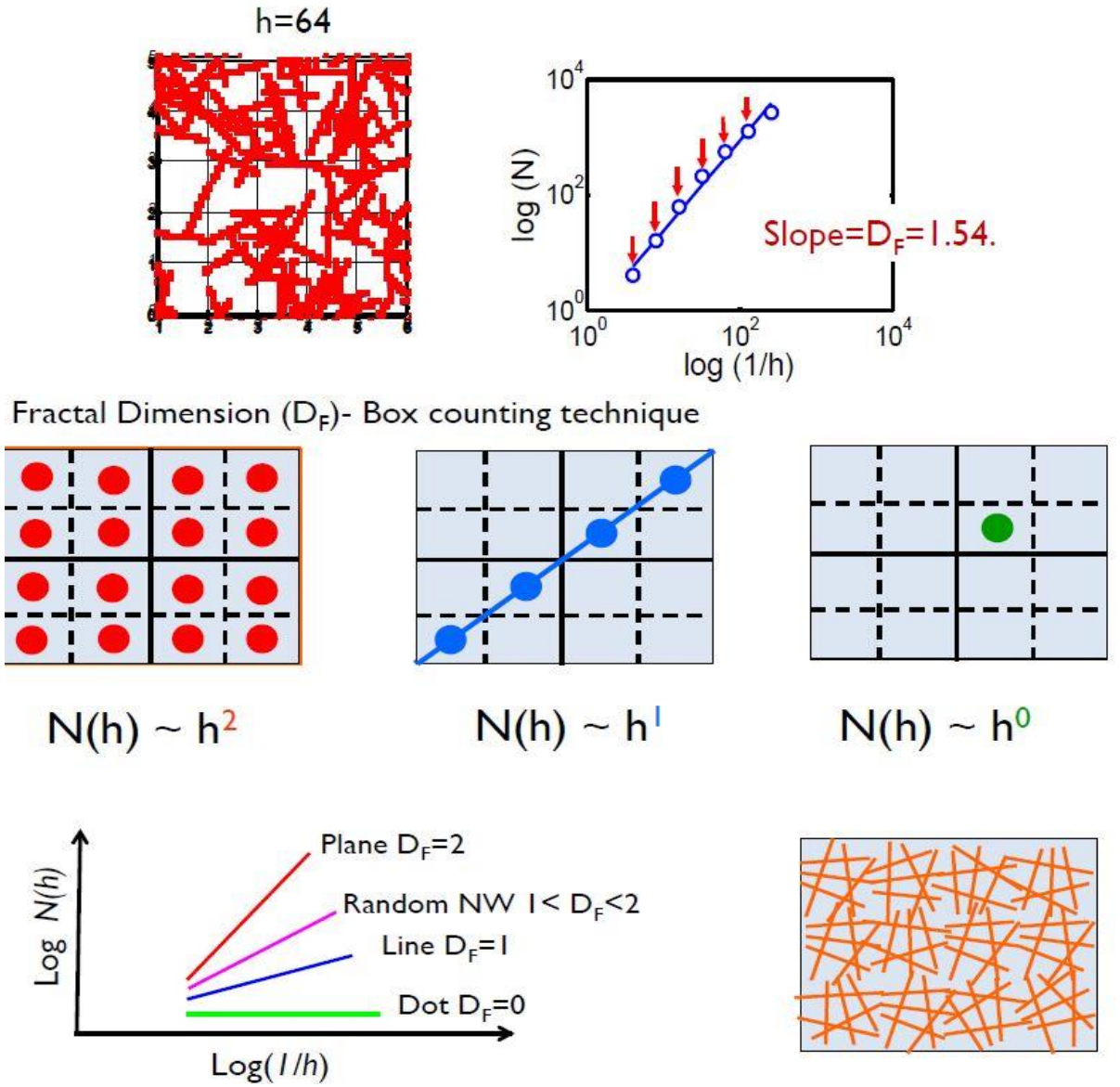

Fig. 19. Fractal Dimension

In case of 2D we see that as we divide the surface the number of cells occupied increases as square so logarithmically plotting we get slope '2'. Again for one dimensional surface the no. of cells occupied increases with slope '1'. For a dimensionless surface no matter how many times we divide only one cell will be occupied.

For a nano-web like structure we need to convert the surface into an equivalent array type surface. Then we calculate its fractal dimensions. At first we find out the fractal dimension of the irregular structure say $D_F = 1.5$. Then we find out the value of 'n' by choosing a value of m.

General algorithm:

For $D_F = 1.5$. Let us calculate n for m = 2 by following formulae:

$$log\ (n) = log(m)/D_F - 1.$$

We get value of n = 4. Next we take a line segment removing the fraction (n-2)/n from center (result = 1/2) and repeat the process.

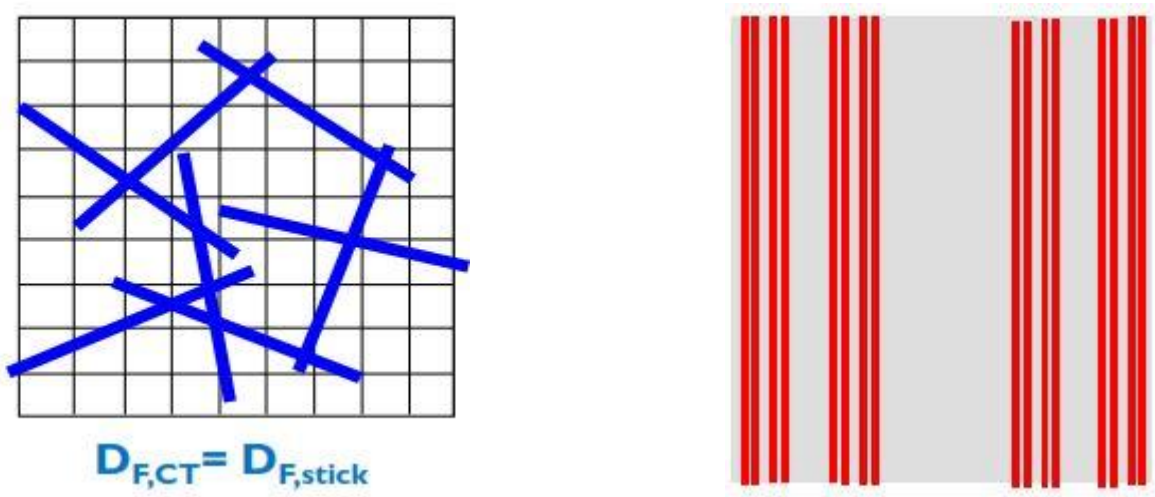

Fig. 20. Fractal Dimension Arrangement

4.3 The Debye-Huckel Screening Effect

The sensing mechanism of an FET sensor is based on the conductance change in the active sensing channel of the FET device due to the interfering electric field/potential imposed by the charged targets. In biosensing measurements, the FET device is mainly dipped in an aqueous electrolytic environment of physiological buffer.

Because of the electrolytic medium, the interaction potential toward the FET sensing channel, exerted from the captured target charges, is attenuated according to the Debye – Huckel screening effect:

$$V(r) = V(r_{bs})e^{\frac{-r_{bs}}{\lambda_D}}$$

Here, r_{bs} = Distance of the target–receptor binding site to the SiNW surface

λ_D = The Debye–Huckel length.

$$\lambda_D{}^2 = \frac{\chi_w \varepsilon_o k_b T_L}{2z^2 I_o N_{av} q^2}$$

Where, ε_o = the vacuum permittivity,

ε_r = relative permittivity of the medium,

k_b = Boltzmann's constant,

T_L = the absolute temperature,

N_{AV} = Avogadro's number,

q = the elementary charge.

The ionic strength (I) of the surrounding buffer solution can be calculated from

$$I = \frac{1}{2}\sum_{i=1}^{n} C_i Z_i^2,$$

Where,

C_i = the molar concentration (M, mol L1) of the ion i,

Z_i = the charge number of that ion, and the sum is taken over all the ions in the buffer solution.

Governed by Debye- Huckel Length's equation, a buffer solution with a higher ionic strength (e.g., high salt buffer) has a shorter λd, thus causing a more severe screening effect on the FET-based sensing measurements.

Screening reduces the distance the sensor can see. Beyond λ_D the sensor cannot detect anything. Screening not only leaves little amount of charge for the sensor but also reduces the effective total charge of the biomolecule. λ_D = length up to which enough salt to neutralize biomolecule. Increase in salt concentration I_0 reduces the distance the sensor can see.

4.4 Reusable Device System

4.4.1 Glutathione (GSH)/glutathione S-transferase (GST)-tag

- A SiNW-FET is first immobilized with GSH to form a GSH/SiNW-FET device, which can then be used to bind GST-fusion proteins.
- At the end of each measurement, the captured protein–GSTs are eluted with a high concentration of GSH solution (>1 mM) to return the device to its original state, making the GSH/SiNW-FET a reusable biosensor.

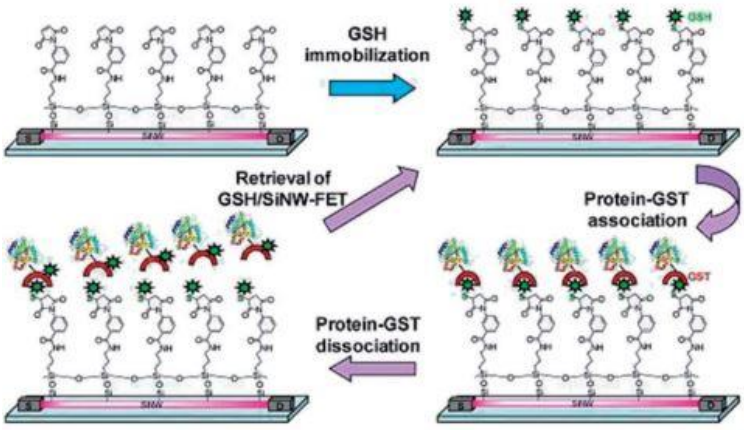

Fig. 21. GSH/GST Tag

4.4.2 Ni2+/ hexahistidine (His6)-tag

- Surface modification is done by (3-glycidyloxypropyl) trimethoxysilane and N-(5-amino-1-carboxypentyl) iminodiacetic acid which binds His6-tagged proteins in the presence of Ni2+.

After the binding, the His6-tagged proteins can be removed by flushing with imidazole or ethylenediaminetetraacetic acid (EDTA).

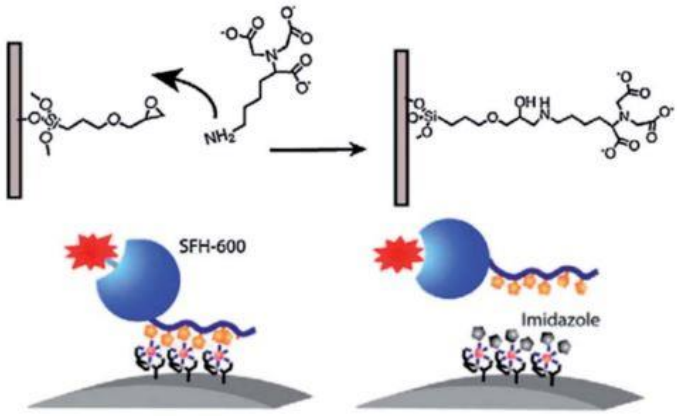

Fig. 22. Ni2+/His6 Tag

4.4.3 A cleavable disulphide bond (S–S) technique

- A SiNW-FET is initially modified with mercaptopropyltrimethoxysilane (MPTMS) to form MPTMS/SiNW-FET by a disulphide bond.
- In biosensing measurements, the antibody captures the targeted virus to form a complex.

After detection, the virus–antibody complex on the SiNW-FET can be removed by cleaving the disulfide bond with dithiothreitol (DTT), thus returning the device surface to its original MPTMS/SiNW-FET.

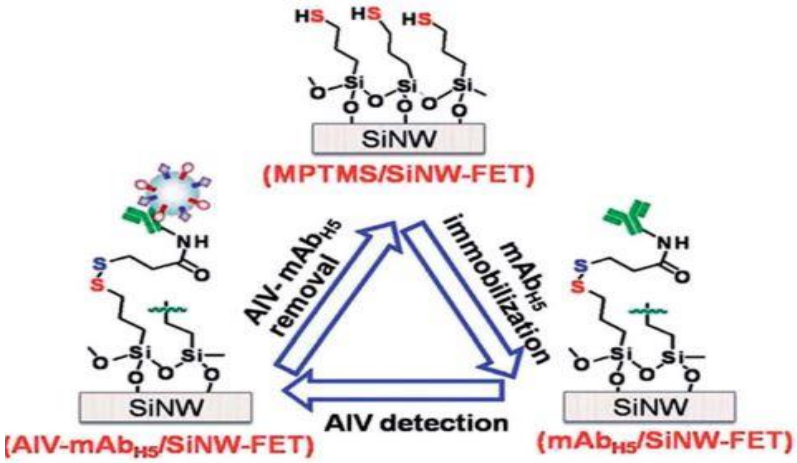

Fig. 23. S-S Technique

4.5 Salt Screening

Normally we would expect the following dependence of drain current to analyte concentration in case of FET sensors:

$$\frac{dN}{dt} = k_F(N_o - N)\rho_s - k_R N$$

$$N_{bio} = \frac{k_F \rho_o N_o}{k_F \rho N_o + k_R} \propto \rho_o$$

$$Q_{Bio} \propto \rho_o$$

$$I = Q_{Bio}\frac{\mu V_D}{L} \propto \rho_o$$

But practically there is salt screening. We need salt (Na+) to bind the two negatively charged DNA which would otherwise rip each other apart. Thus salt takes away some charge. Thus the actual dependence of sensitivity becomes:

$$S(t) \sim c_1\left[\ln(\rho_0) + \frac{(3 - D_F)\ln(t)}{2} - \frac{\ln(I_0)}{2} + \alpha[pH]\right] + c_3$$

It considers the salt concentration and pH consideration. In fact there is a second capacitance (double layer capacitance) formed when the Na+ are pushed towards the surface of biosensor and Cl- are driven away from the surface due to repulsion.

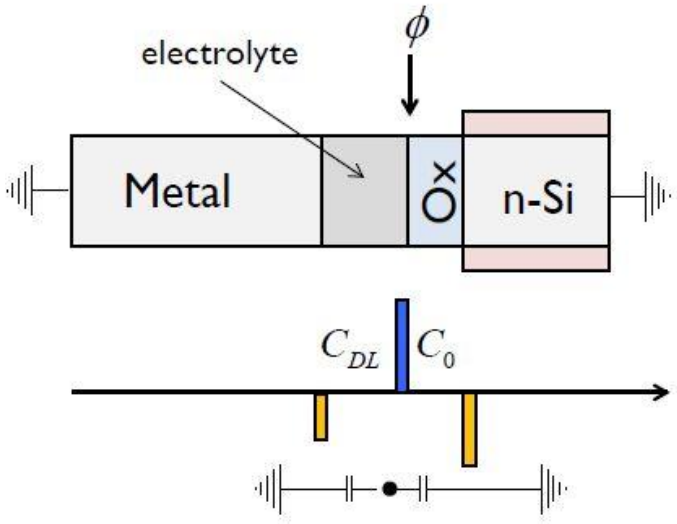

Fig. 24. Salt Screening

$$Q_{bio} = Q_L + Q_R$$
$$= C_{DL}\phi + C_0\phi$$

$$\phi = \frac{Q_{bio}(\mathrm{pH})}{C_{DL}(\mathrm{salt}) + C_0}$$

$$Q_{MOS} = C_0 \frac{Q_{bio}}{C_{DL} + C_0}$$

$$I = Q_{MOS}\upsilon$$

Considering salt concentration to be very high and solving various differential equation, we get the solution for sensitivity. The results are the same for nanowire and planar sensors.

$$S(t) \equiv \frac{\Delta I_D}{I_D} \propto Q_{MOS}$$
$$= c_1 \ln(\rho_0) + c_2 \frac{(3 - D_F)\ln(t)}{2} - c_3 \ln(I_0) + c_4$$

Response logarithmic in density, as observed experimentally

Increases with time, but logarithmically

Increasing salt decreases response

4.6 Effect of fluidic environment

The high k dielectric water spreads the charge over the surface so they get uniformly distributed over the sensor surface.

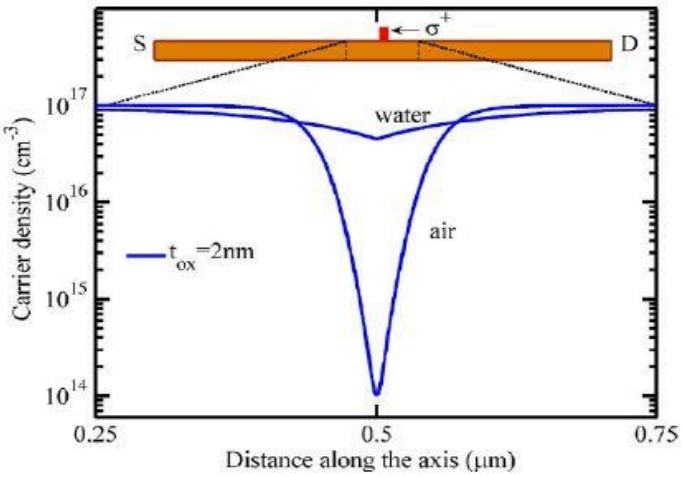

Fig. 25. Carrier Density vs. Distance

4.7 Effect of pH

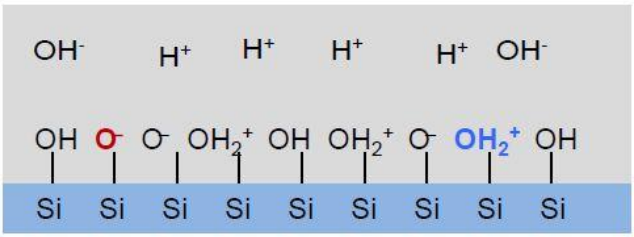

de-protonation

$$SiOH \Leftrightarrow SiO^- + H^+$$

$$\frac{[SiO^-][H^+]_S}{[SiOH]} = K_b$$

protonation

$$SiOH_2^+ \Leftrightarrow SiOH + H^+$$

$$\frac{[SiOH][H^+]_S}{[SiOH_2^+]} = K_a$$

$$Q = q\left([SiOH_2^+] - [SiO^-]\right)$$

$$[H^+]_S = [H^+]_B e^{-q\psi_0/k_BT}$$

The pH of the fluidic environment has a significant effect on the accuracy of detecction. Due to pH charge develops on the surface as we see from the above figure. Spontaeneous reaction occurs at surface of Oxide layer introduces both positive and negative charge. Thus there occurs a net charge on the surface due to pH. We should carry detection in a fluidic environment as such the net charge due to pH is zero. That can be determined in the following way:

$$Q(pH) = qN_0\left\{\frac{[H^+]_S/K_a - K_b/[H^+]_S}{[1 + K_b/[H^+]_S + [H^+]_S/K_a]}\right\}$$

Putting numerator zero we get,

$$K_a K_b = [H^+]_S^2 = [H^+]_B^2$$

$$K_a = 10^{-pK_a}, K_b = 10^{-pK_b}$$

$$pzc = \frac{pK_a + pK_b}{2}$$

There is a Nernst limit for change of gate voltage w.r.t. pH otherwise response wouldn't be precise. It is calculated as 59mV/pH.

4.7.1 Charge of Biomolecules

- **DNA:**

DNA is an acid and acids are charged in solution. Charge of DNA is controlled by pH.

$$[H_3PO_4]_0 = [H_2PO_4^-] + [HPO_4^{2-}] + [PO_4^{3-}]$$

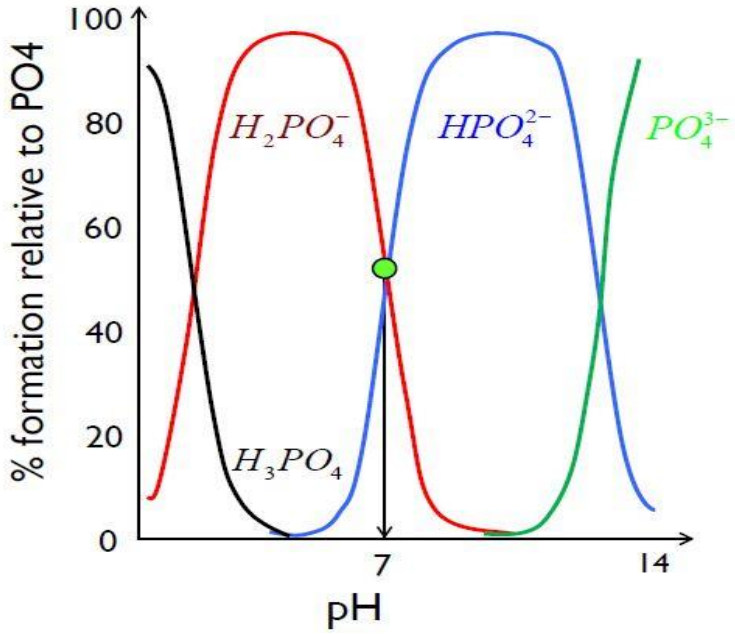

Fig. 26. Formation vs. pH

- **Protein:**

Protein involves charged residue. Charge of a protein can be positive or negative. Protein is composed of 20-Amino Acid. Of them, 7 are charged. Protein detection should be done at pH away its isoelectric point. At isoelectric point the charge is zero for a definite protein.

$$Q = q(N_{term} + \alpha K + \beta R + \gamma H + \delta D + \varepsilon E + \xi C + \eta Y + C_{term})$$

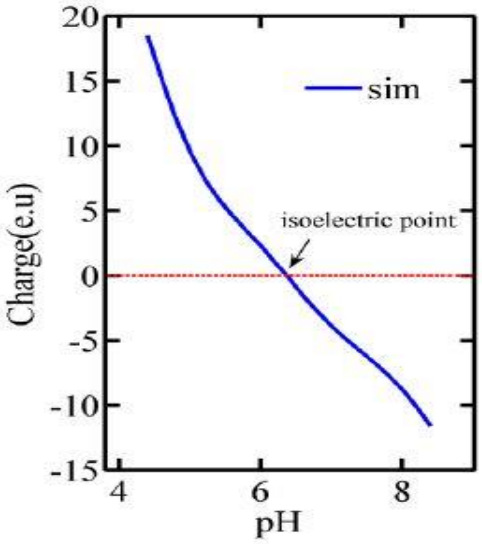

Fig. 27. Charge vs. pH

4.8 Techniques to overcome screening

- De-screening of DNA at high frequencies.
- Sensors with giant Nernst Response amplifies signal electronically to improve sensitivity to pH changes. However, SNR is improved only for special case.
- Amperometric and cantilever sensors do not suffer from screening limits (but diffusion limit still applies).

Chapter 5

Settling Time of Nanowire Biosensors

5.1 A fundamental relationship for Nanobiosensors

The time required for minimum no. of biomolecules to detect confidently is called settling time of the nanobiosensor. The following is the very fundamental relation that a nanobiosensor obeys,

$$\rho * t^{\frac{3-D_F}{2}} \sim C$$

Where, ρ = density of the analyte

t = settling time

D_F = Fractal Dimension.

The denser the medium, the quicker the detection becomes. Again, the longer we wait for the detection, the lesser the density of analyte we need. This comes from the very basic energy-time relationship of Heisenberg,

$$\Delta E \times \Delta t \sim C$$

The more time we take more precise detection of energy we can make.

5.2 Dimensional dependence of settling time with Dimension

5.2.1 Considering simple geometry

For determining dimensional dependence of settling time with dimension, the diffusion capacitance approach is preferable. We observe the steady state (state where no. of biomolecules attached remains fixed. Biomolecules charge depends on flux and capacitance and on permittivity or diffusion coefficient D.

Transient response $N(t) = C_{D(t)} \rho_0 t$

$$C_{D(t)} = \frac{D}{\sqrt{2Dt}} \qquad C_{D(t)} \sim \frac{2\pi D}{\ln\left(\sqrt{4Dt}/a_0\right)} \qquad C_{D(t)} \sim \frac{4\pi D}{a_0^{-1} - \left(1/\sqrt{6Dt}\right)}$$

$$N(t) = k\rho_0 t_s^{1/2} \qquad N(t) = k\rho_0 t_s^{1} \qquad N(t) = k\rho_0 t_s^{1}$$

Steady State: Analogy to Electrostatics

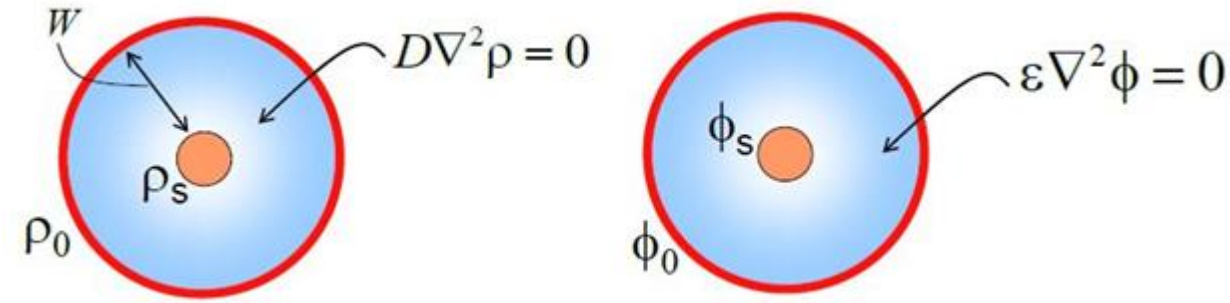

Fig. 28. Analogy to Electrostatics

$$I = C_o(\rho_0 - \rho_s)$$

$$C_0 = \frac{D}{W} \text{ (Planar)}$$

$$= \frac{2\pi D}{\log(\frac{W+a_0}{a_0})} \text{ (NW)}$$

$$= \frac{4\pi D}{a_0{}^{-1} - (W+a_0)^{-1}} \text{ (ND)}$$

$$Q = C_0(\emptyset_0 - \emptyset_s)$$

$$C_0 = \frac{\varepsilon}{W} \text{ (Planar)}$$

$$= \frac{2\pi\varepsilon}{\log(\frac{W+a_0}{a_0})} \text{ (Cylinder)}$$

$$= \frac{4\pi\varepsilon}{a_0{}^{-1} - (W+a_0)^{-1}} \text{ (Sphere)}$$

Applying the diffusion capacitance approach the result is close to the exact solution. It gives similar relationship as the exact equations. From various readings the plotted data of settling time vs. diffusion from experiment and from equation are approximately same.

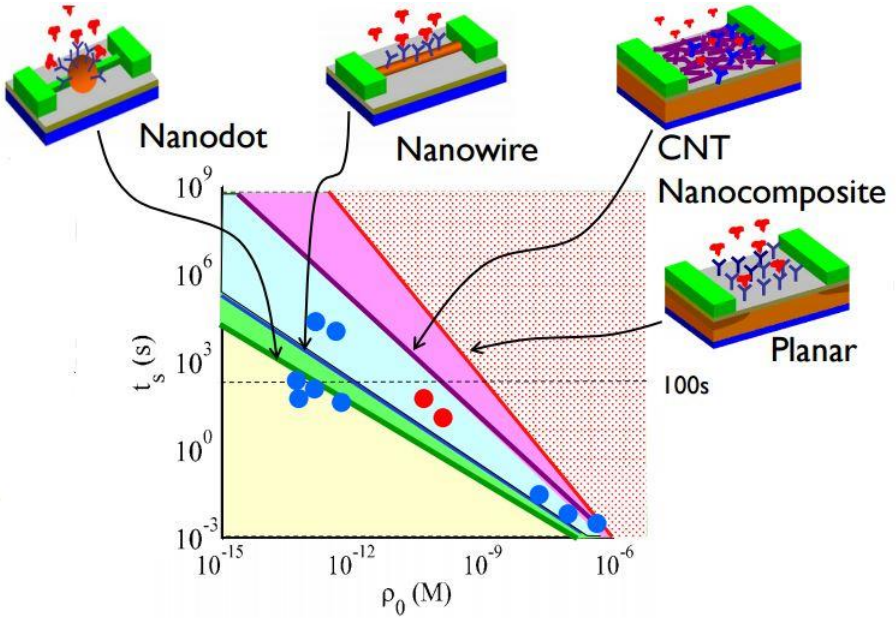

Fig. 29. Settling time vs. concentration

From the graph it seems that the nanowire sensors and nanodot sensors show almost similar performance which is inevitable from the relation as well.

5.2.2 Considering complex geometry

- **Array type sensor:**

For more complex geometry, things are not simple. For array of nanowire, initially the surface looks like planar but as the diffusion front approaches the cylindrical nanowires act as 1D sensors. We take a look at capacitance of array of wires and an electrode. The distance between electrode and wires is not constant.

$$N(t) = C_{D(t)}\rho_o t$$

$$C_{D(t)} = \frac{2\pi D}{\log\left[\frac{\sinh(2\pi\sqrt{2Dt}P)}{\pi a_0 P}\right]}$$

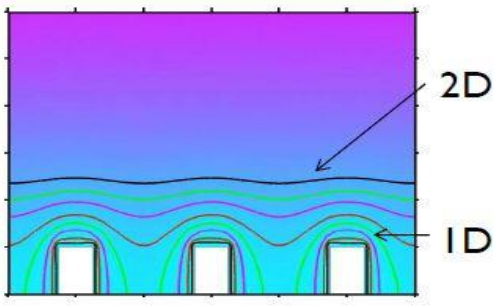

Fig. 30. Array type sensor

As the flux of molecules approach the sensor surface the sensors looks like a 2D surface. As the time progresses flux of biomolecules recognize individual nanowires and the dimension dependence is like that of a 1D.

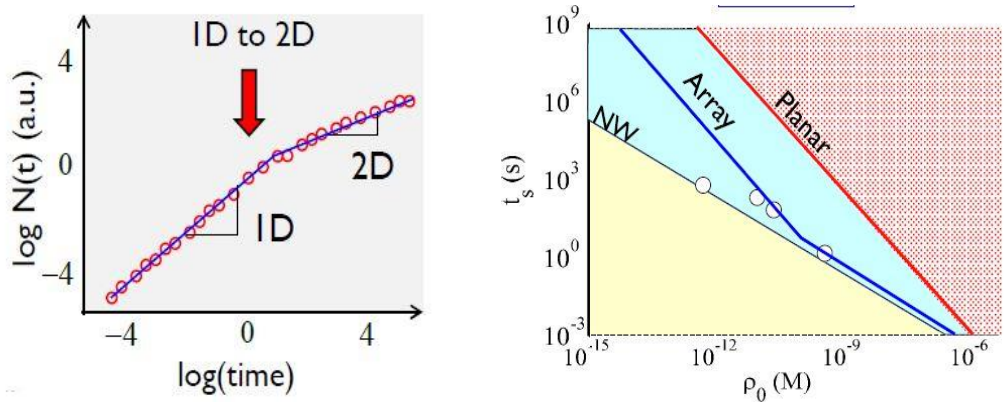

Fig. 31. log N(t) vs. log(t)

- **Nano-Composite type sensor:**

For nano-composite type sensors we need to convert the complex geometry into equivalent array type structure. Here the dimentional relationship shifts from 2D to 1D and then again from 1D to 2D.

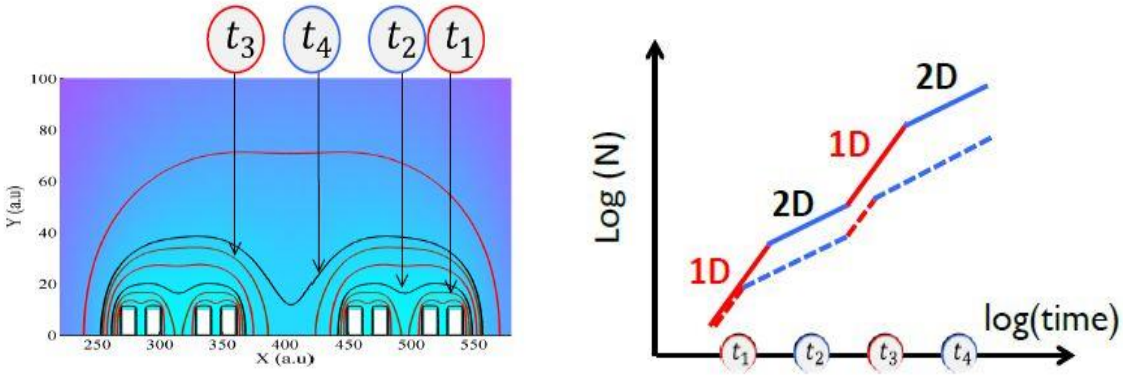

Fig. 32. Nano-Composite type sensor

5.3 First Arrival time vs. Ensemble average

When we look at a plot of linear line showing the settling time vs analyte density we are actually looking at an ensemble average. All the sensors might not have captured a biomolecule. Thus we might misinterpret the sensing limit of the technology. So we have to wait until all the sensors have responded.

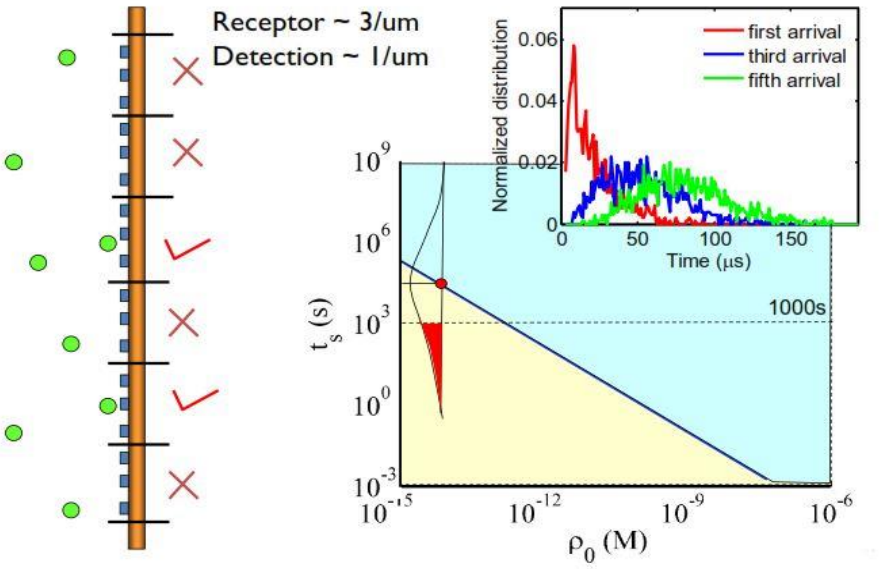

Fig. 33. Arrival vs. Ensemble average

In order to find out the average we must wait until we get response from all the sensors. So for a biomolecule to travel a length 'L' on average it takes,

$$t \sim L^2/D$$

Chapter 6

Materials used as channel

Table 6.1 Different nanomaterials used as channel

Sl. No.	Nanomaterials Used	Types of materials	Advantages
1	Carbon Nanotubes	1-D	➢ Improved enzyme loading, ➢ higher aspect ratios, ability to be functionalized ➢ better electrical communication
2	Nanowires	1-D	➢ Highly versatile, ➢ Good electrical and sensing properties for bio and chemical sensing; ➢ Charge conduction is better.
3	Nanorods	1-D	➢ Good plasmonic materials which can couple sensing phenomenon well ➢ Size tunable energy regulation, ➢ Can be coupled with MEMS, and induce specific field responses
4	MoS_2 flakes	2-D	➢ Greatly advantageous for biosensor device scaling without compromising its sensitivity, ➢ highly flexible and transparent nature, ➢ can offer new opportunities in advanced diagnostics and medical prostheses
5	Graphene	2-D	Graphene is an ideal material for the construction of FET biosensors because

			➢ it is a zero-band gap semiconductor ➢ the band gap can be tuned by surface modification
6	Graphene Quantum Dot	0-D	

6.1 2-D materials

The materials with 2D structure such as CNT, MoS_2 and Graphene, due to their atomically thin structures can provide excellent electrostatics and also because of possessing planar nature they are suitable to large-scale fabrication and integrated device processing. A MoS_2- based pH sensor achieving sensitivity as high as 713 for a pH change by 1 unit along with efficient operation over a wide pH range (3–9) is demonstrated. Chen, Li, and co-workers demonstrated that large-scale chemical vapor deposition (CVD) grown single- and few-layer graphene films are highly sensitive to DNA hybridization. Graphene has been employed in many schemes for sensing glucose.

6.2 1-D materials

6.2.1 Carbon Nanotubes

Since their discovery in 1990's, they have attracted researchers all over the globe in nanobiosensing due to high electron conductivity, mechanical strength and folding abilities. Both single walled and multiwalled have been used in biosensing. Carbon nanotubes have also been used for enhancing the electrical detection of the sensing phenomenon, owing to their better and smoother electron transfer flow characteristics. The functionalization of carbon nanotubes and their rapid friendliness for being coupled with biomolecules like DNA, proteins, oligonucleotide probes have already been achieved.

6.2.2 Nanowires

Nanowires are the one dimensional nanostructures with very good electron transport properties. In a study, silicon nanowires coated with biotin have been used for the detection and isolation of streptavidin molecules from a mixture. Silicon nanowire FET have been used to detect cardiactroponin, dengue virus, DNA detection MicroRNA [label-free and ultrasensitive detection of microRNA biomarkers in lung cancer cells based on silicon nanowire FET biosensors], PSA. Enzyme coated ZnO nanowires have been used to detect uric acid. Besides ZnO nanostructures are found to be used in bio sensing. Reports in TiO_2 nanowires in nanobiosensing is available. Moreover Gallium Nitride nanowire devices are being used in nanobiosensing.

6.2.3 Nanorods

ZnO nanorods have been used to detect glucose. Tin oxide nanorod assays have successfully been used Hydrogen peroxide` detection. Gold nanorods have been used for enzyme-free detection of biomolecules. An electrochemical DNA biosensor based on gold nanorods decorated Graphene oxide sheets for sensing platform has been realized.

6.3 0-D materials

Graphene quantum dots (GQDs), as defined, are a kind of 0D material with characteristics derived from both Graphene and CDs, which can be regarded as incredibly small pieces of Graphene. Li et al. designed the first electrochemical sensors using GQDs based on the strong interaction between single-stranded DNA (ssDNA) and GQDs. Ai and co-workers designed a novel sandwich-type electrochemical immunosensor with a Fe_3O_4 at GQDs hybrid and apoferritin-encapsulated Cu (Cu-apoferritin) nanoparticles as labels for highly selective and sensitive detection of avian leukosis virus subgroup J (ALVs-J). Moreover, the detection of H_2O_2 in living cells was realized by using this GQDs/Au electrode.

Chapter 7

A Comparative Study of Electrical Properties of Si and ZnO Gate-all-around Nanowire FET

7.1 Abstract

A comparative study of various electrical properties of n-channel Gate-all-around (GAA) Si and ZnO nanowire Field-Effect Transistors has been assessed and presented. The simulation results shown here are based on self-consistent solution of energy balance equation. The temperature, channel diameter and gate length dependence of various electrical parameters like subthreshold swing (SS), threshold voltage and transconductance have been simulated. ZnO nanowire FET showed better threshold voltage but poor subthreshold swing and transconductance with respect to Si nanowire FET.

7.2 Insight

Transistors are used widely as fundamental building element in today's electronic circuits. For the past 30 years MOS devices have been improving at a dramatic speed [74]. As predicted by Moore's law, the dimension of transistors is shrinking smaller and smaller into nanoscale. Scaling of transistor dimensions has great impact on information processing system. Scaling of transistor causes few technical problems [75].

FinFET and Silicon on insulator (SOI) technology are disadvantageous as channel width variations may result into mobility loss. But Gate-all-around (GAA) technology can overcome these limitations and become a better technology for FET. GAA FET is a nanowire structure in which a gate is placed on all four sides of the channel. One of the key challenges of building future nanoscale transistors is ensuring good gate control over the channel. GAA FET is very much able to comply with that.

Prerequisite to grasp the working method of any sort of solid state devices is extensive knowledge on device physics. To understand device physics in depth and to assess the performance limits of NWTs, simulation is becoming increasingly important. Simulation tools can support experimental work to accelerate the FETs [76], reduce their cost, identify their strengths and weaknesses, and demonstrate their scalability down to the nanometer range [77-78].

7.3 Need and Scope of present study

ZnO is one of the most prominent II-IV semiconductors that have been investigated since the early 1930s [79-80]. ZnO is a wide bandgap material with a direct bandgap of about ~3.4eV [81]. It preferentially crystallizes in the hexagonal wurtzite type structure [81]. The large bandgap and possibility of introducing n type dopants easily makes ZnO an attractive choice for transparent conductors and transparent FET [82]. The modulation of bandgap over wide range by alloying cadmium and magnesium has been successfully demonstrated for UV-optoelectronics [79]. ZnO nanoparticles and nanowires have been used as electron transport layer in dye-sensitized solar cell [83-84]. Development of 1-D ZnO nanostructures as

biosensors is in the embryonic but potential stage [85-90]. Various enzymes have been immobilized in order to realize highly selective bioassays [91-93]. Surface modification of ZnO nanowires with biotin for streptavidin detection has been done [94]. Enzyme coated ZnO nanowire FET have been used in uric acid detection [95]. Further ZnO nanowire for DNA sensory applications can be found in literature [96].

During the last decade, there have been several studies concentrating on the development of Si-based nanowire sensors [97-99] Si nanowires are CMOS compatible [100]. Although ZnO nanowire are not CMOS compatible but ZnO is very stable under ambient conditions and oxygen rich environment [101-103]. Si-NWT has been in the center of attraction for many decades due to availability and ease of fabrication. But as time progressed the industry saturated and the need for better and efficient material for nanowire FET has grown. Thus ZnO can provide a good alternative. But there can be a little amount of work found on ZnO nanowire based devices. In this paper, a comparative simulation based study of different parameters has been provided considering the importance and increasing demand of Si and ZnO nanowire transistors in different applications.

7.4 Device structure and Simulation methodology

The device structure of Gate-all-around n-channel nanowire FET structure has been illustrated in Fig. 1, which consists of Oxide Thickness *Tox*, channel diameter *Dch*, gate length *Lg*, source length *Ls*, drain length *Ld*, gate overlap to source *Os*, gate overlap to drain *Od*. Further, the oxide is placed on either sides of the side walls of the FET. The thickness of the side wall oxide is specified by *tox*1 and *tox*2. For simulation purpose, source and drain lengths were both chosen 100nm and the gate length has been varied in the range of 500 nm to 800 nm, channel diameter from 20 nm to 60 nm. The oxide thickness has been taken 10 nm and kept constant throughout the simulation studies. The drain and source doping has been kept fixed at 2×10^{24} cm^{-3} and channel doping was 8×10^{16} cm^{-3}. The gate bias was varied from -1.5 V to 2 V whereas drain bias has been kept at 0.8V. Oxide overlap has not been considered.

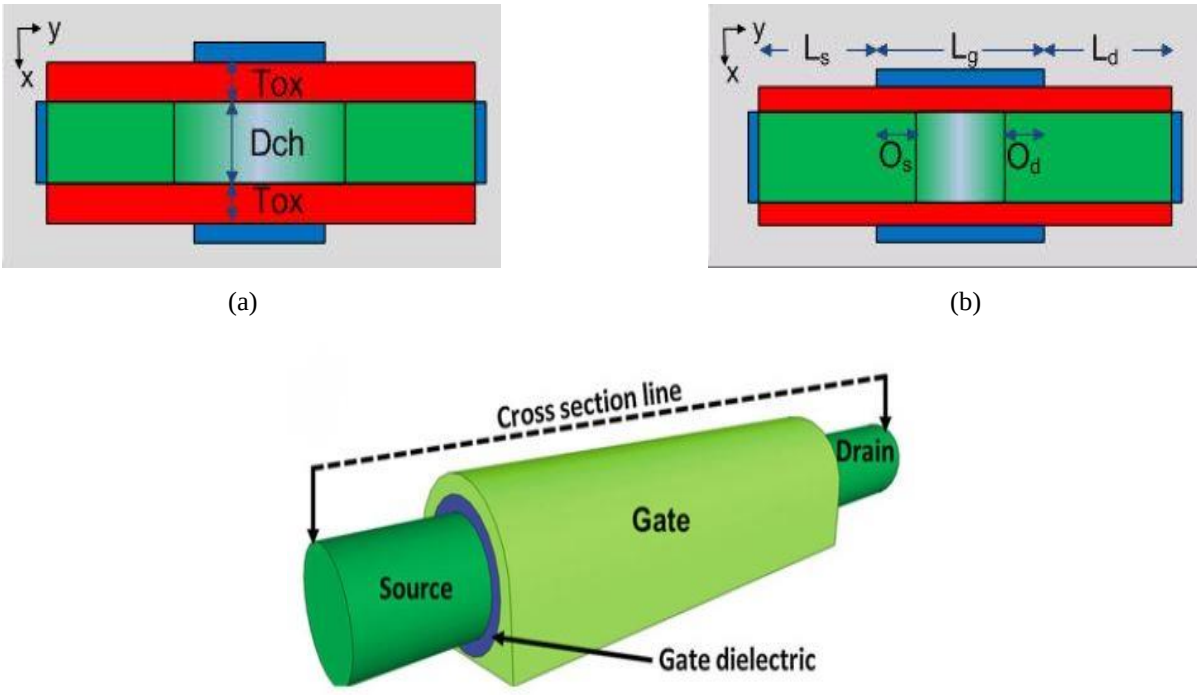

Fig. 34**.** Two Dimensional structure of Gate-all-around Nanowire FET device (a) for geometry- x [104] (b) for geometry- y [104] (c) Quasi-planar three dimensional structure of Gate-all-around Nanowire FET device [105]

The simulation tool MuGFET was used to investigate various effects of the NW parameters like temperature, gate length and channel diameter on NWT *I–V* characteristics. The MuGFET software was designed and developed at Purdue University. MuGFET is a simulation tool for nanoscale multi-gate FET structures [104]. From MuGFET, PADRE simulator was used which was developed by Bell Laboratories. PADRE is mainly device oriented simulator for 2D/3D device with arbitrary geometry. It provides many useful plots which comes useful for deep understanding of device physics and operation. MuGFET provides self-consistent solutions to the Poisson and drift-diffusion equations and is used to simulate ballistic transport in the calculation of the characteristics of NWTs [106].

Table 7.4 List of various properties of Si and ZnO channel materials at 300K undertaken for simulation study

S. No.	**Properties**		**Si [107]**	**ZnO**
1	Energy band-gap (eV)		1.12	3.37[108]
2	Dielectric constant		11.7	8.49[109]
3	Electron affinity (V)		4.05	4.35[108]
4	Electron effective mass		$0.2m_o$	0.26[110]
5	Light Hole effective mass		$0.16m_o$	$0.59m_o$[110]
6	Heavy Hole Effective mass		$0.49m_o$	$0.59m_o$[110]
5	Density of states effective mass	Electrons	$1.18m_o$	$0.29m_o$[111]
		Holes	$0.81m_o$	$1.21m_o$[111]
6	Electron mobility (cm^2/V-s)		1450	300[112]
7	Hole mobility (cm^2/V-s)		500	5[113]
8	Saturation Velocity (cm/s)	Electrons	1.0×10^7	2.24×10^7 [114]
		Holes	0.704×10^7	3.4×10^5 [114]

7.5 Simulations and Results

7.5.1 I_d vs. V_g curves for ZnO and Si

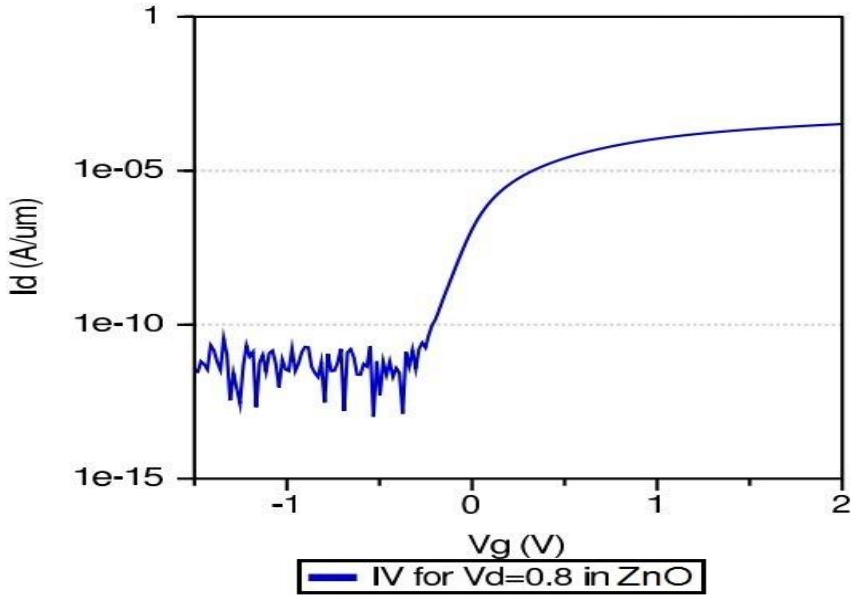

(a)

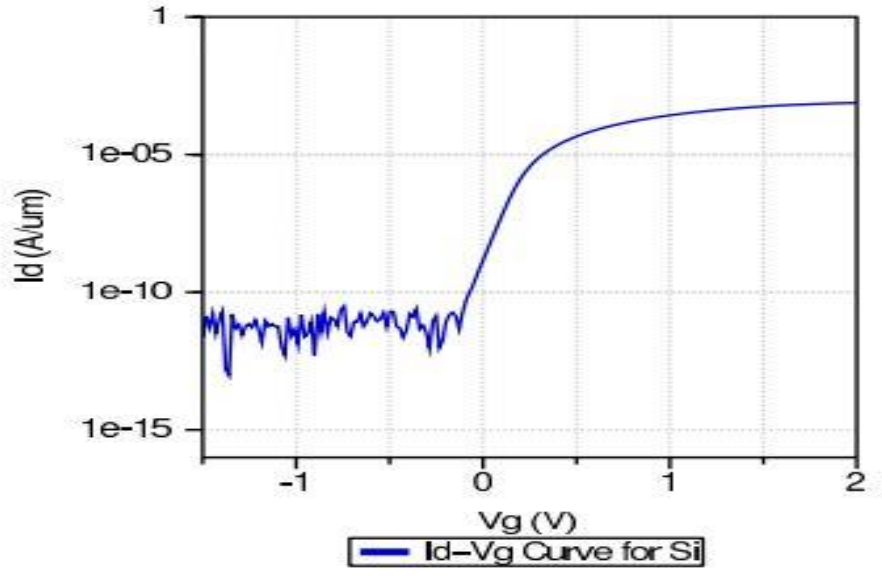

(b)

Fig. 35 (a) I_d vs. V_g curve for ZnO (b) I_d vs. V_g curve for Si

In fig. 35, it is shown that the normalized Id-Vg graph for ZnO with moderately doped channel at 300K was simulated. It is observed from the graph that the on/off current ratio is about 10^6. The threshold voltage was obtained to be 0.394V and subthreshold swing was found to be 113.891 mV/decade. The simulation results were fairly in consonance with the experimental data for ZnO nanowire FET [115]. The gate length was chosen 800nm and diameter was fixed at 60nm for both ZnO and Si.

7.5.2 Subthreshold Swing vs. Temperature, Channel Diameter and Gate Length

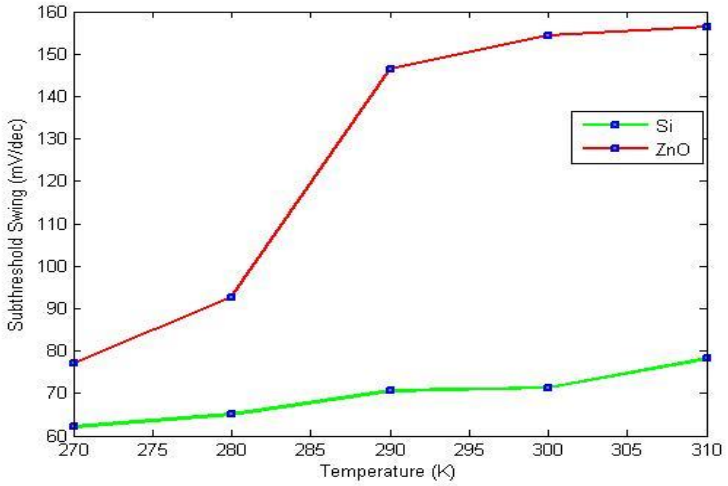

(a)

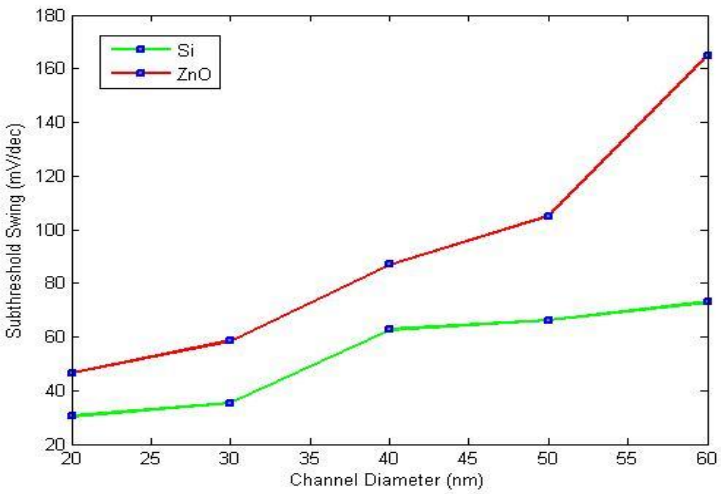

(b)

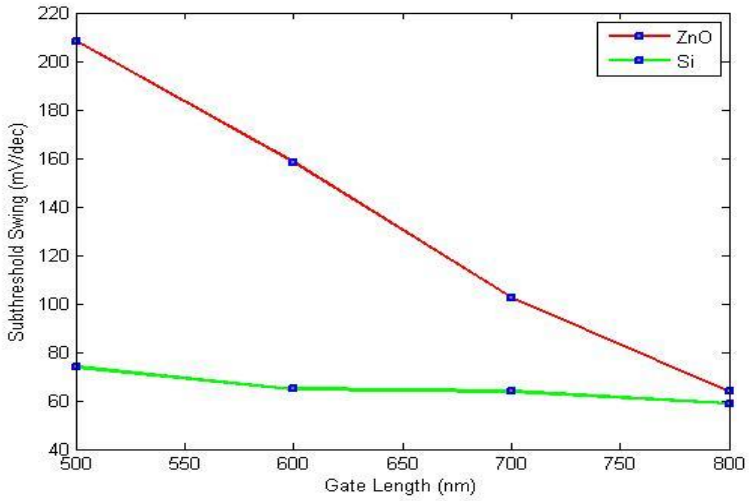

(c)

Fig. 36. (a) Subthreshold Swing vs. Temperature (b) Subthreshold Swing vs. Channel Diameter (c) Subthreshold Swing vs. Gate Length

Subthreshold swing gives insight of the leakage currents associated with the device characteristics. Several studies suggest that subthreshold swing of ZnO nanowire FET being very high which complies with our result [115-116]. Small subthreshold swing means better channel control and improved I_{on}/Io_{off} which usually means less leakage, and less energy.

In Fig. 36 (a), it has been observed that subthreshold swing increased with temperature as expected. At room temperature ZnO showed much worse subthreshold swing compared to Si. In Fig. 36 (b), subthreshold swing vs. channel diameter was plotted. The subthreshold swing increased for both Si and ZnO, ZnO showing higher subthreshold swing. Similarly, in Fig. 36 (c) subthreshold swing vs. gate length was plotted. The subthreshold swing of Si was quite stable at all gate length whereas subthreshold swing of ZnO decreased steeply. At long gate length ZnO and Si showed similar subthreshold swing.

7.5.3 Threshold Voltage vs. Temperature, Channel Diameter and Gate Length

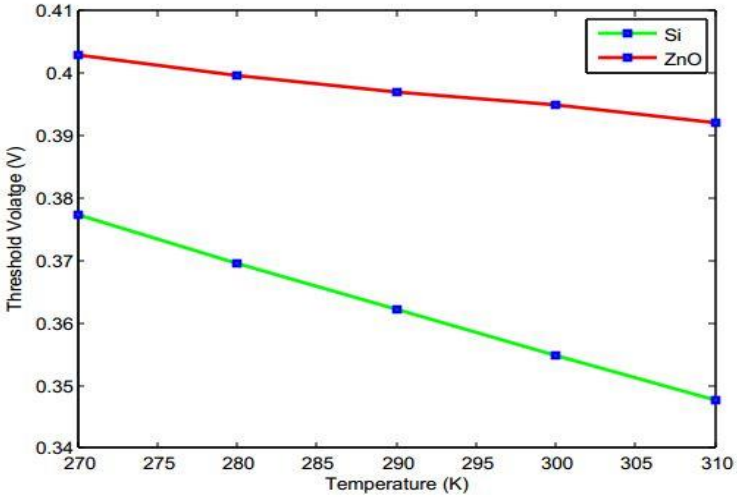

(a)

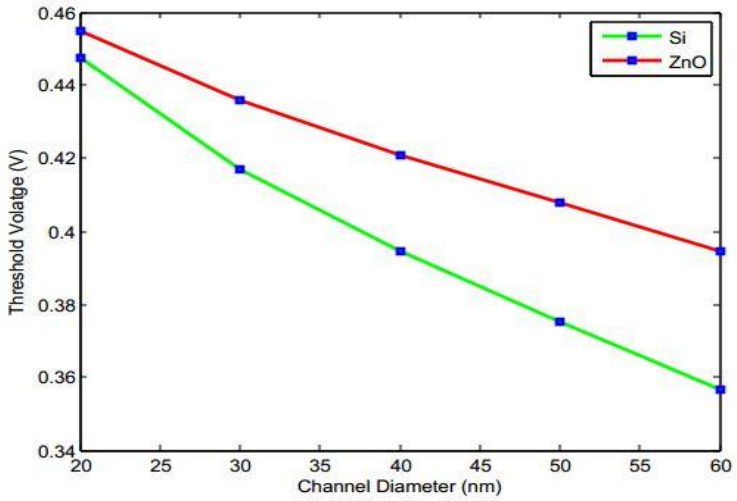

(b)

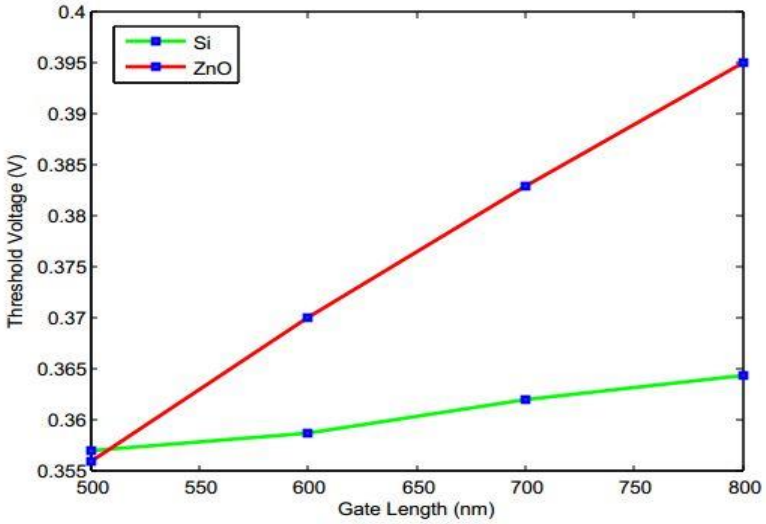

(c)

Fig. 37. (a) Threshold voltage vs. Temperature (b) Threshold voltage vs. Channel diameter (c) Threshold voltage vs. Gate length

The threshold voltage is an integral technological parameter that should be maintained properly for a nanowire device. In fig. 37 (a), by varying temperature from 270K to 310K, the change observed in threshold voltage in ZnO was found less steep than Si. ZnO provided higher threshold voltage than Si. In fig. 37 (b), this was also true for channel diameter while the diameter was varied from 20 nm to 60 nm. In fig. 37 (c), with the increase of gate length, threshold voltages increases. As the distance between the drain and source decreases, potential becomes more pronounced to drain electric field encroachment leading to an earlier threshold point of gate bias. Although the initial value for ZnO was lower than Si, the value of threshold voltage of ZnO increased very steeply with the increase of gate length. In all cases, Si offered worse threshold voltages. Lowering this threshold tends to result in the channel never being fully switched off – it's always leaking some current. From this perspective ZnO would be preferable for most logic application. However for low power device power efficiency is obtained by lowering threshold where Si would be useful.

7.5.4 Transconductance vs. Temperature, Channel Diameter and Gate Length

Transconductance, g_m, is a measure of the sensitivity of drain current to changes in gate-source bias. The transconductance of the MOSFET decides its gain and is proportional to hole or electron mobility for low drain voltages. In this simulation, ZnO has shown a lower transconductance with respect to Si which is obvious due to low electron mobility. So Si-NW FET are more sensitive than ZnO in this regard. In this simulation, normalized transconductance was plotted.

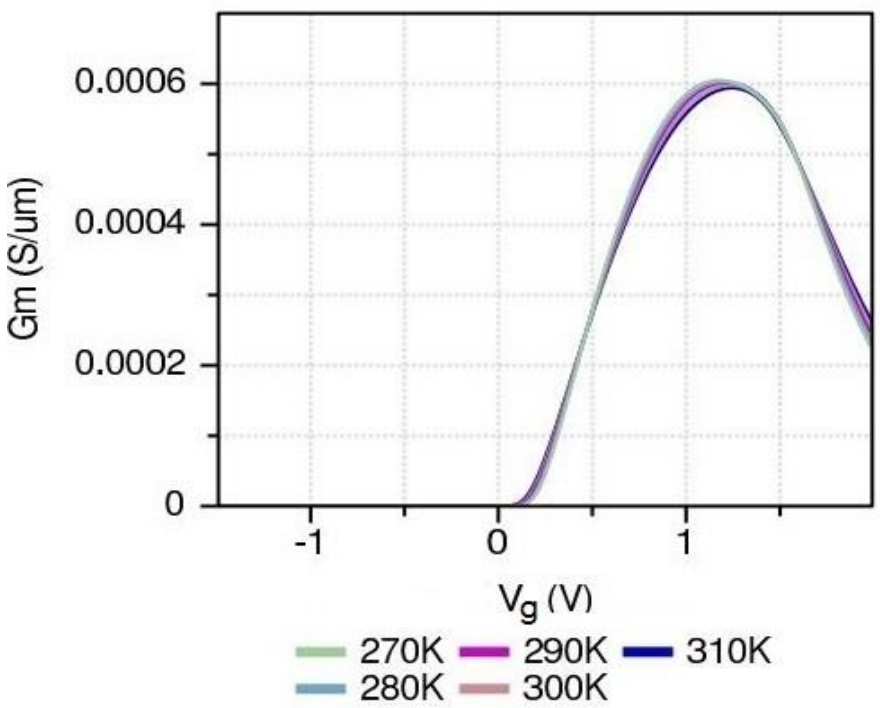

(a)

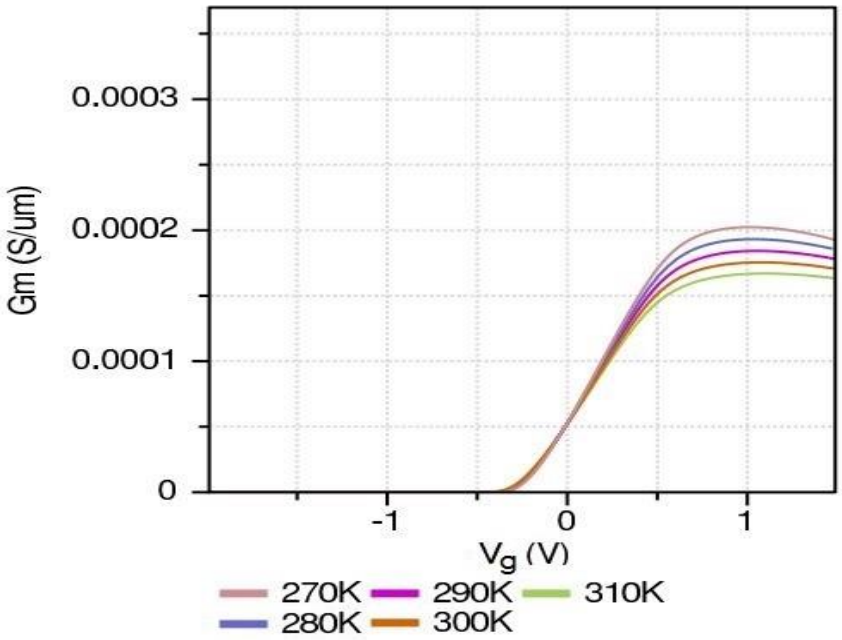

(b)

Fig. 38. (a) Transconductance vs. Temperature for Si (b) Transconductance vs. Temperature for ZnO

In fig. 38(a) and fig. 38(b), by varying temperature from 270 to 310K, it was observed that the highest transconductance was achieved near about 1.2V. The transconductance for Si nanowire was quite stable. For ZnO, highest transconductance was achieved near about 0.8V.

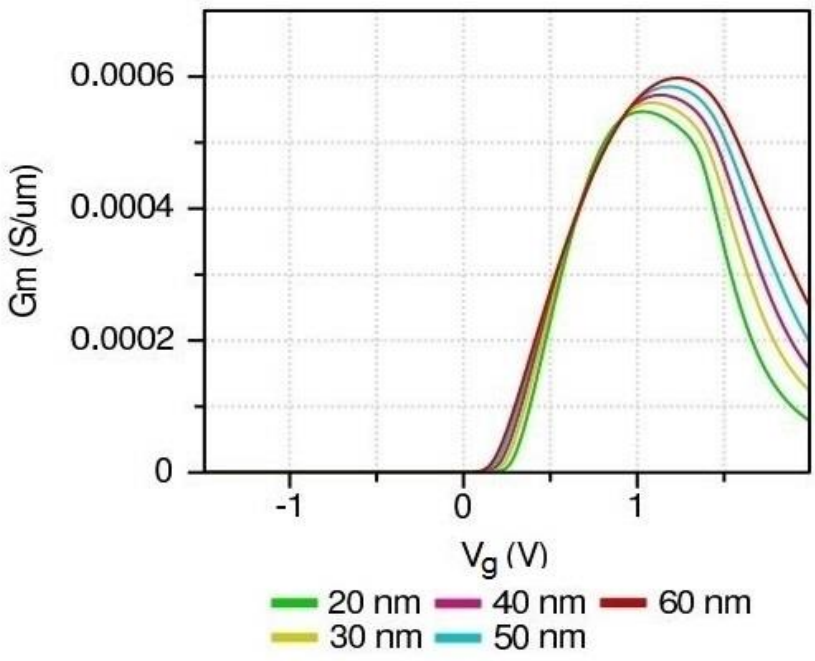

(a)

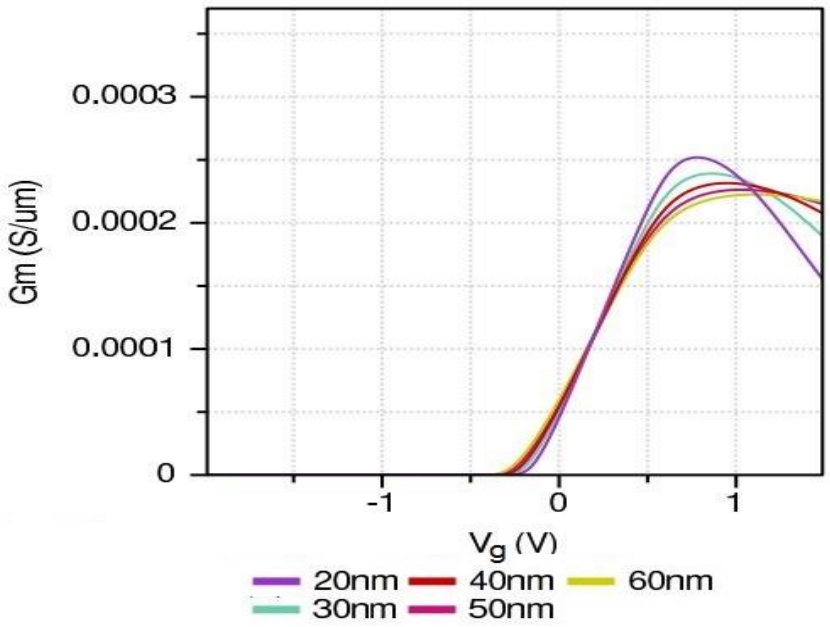

(b)

Fig. 39. (a) Transconductance vs. Channel Diameter for Si (b) Transconductance vs. Channel Diameter for ZnO

In fig. 39 (a), it is shown that for Si, with the decrease in channel diameter, the highest transconductance was decreased and shifted to the right. In fig. 39 (b), it is shown that for ZnO, the highest transconductance increased with the decreasing in diameter and shifted to the left.

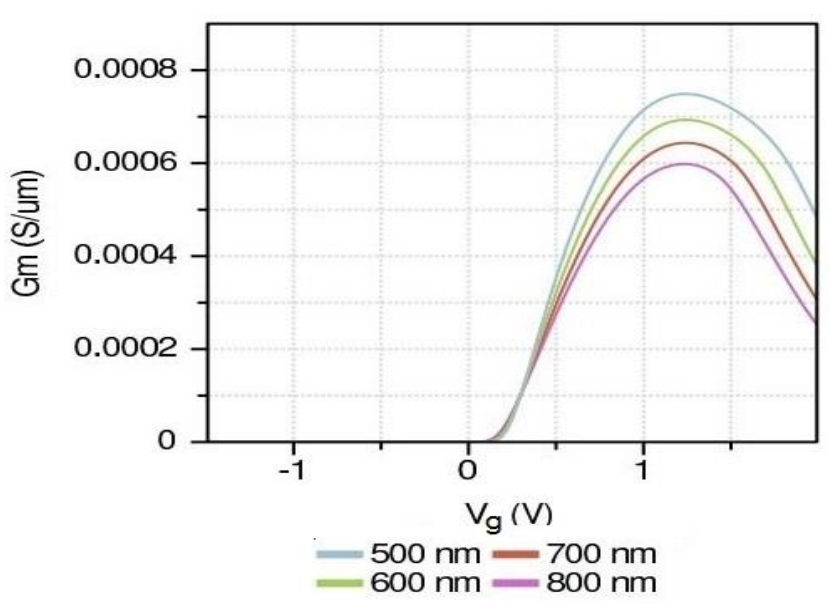

(a)

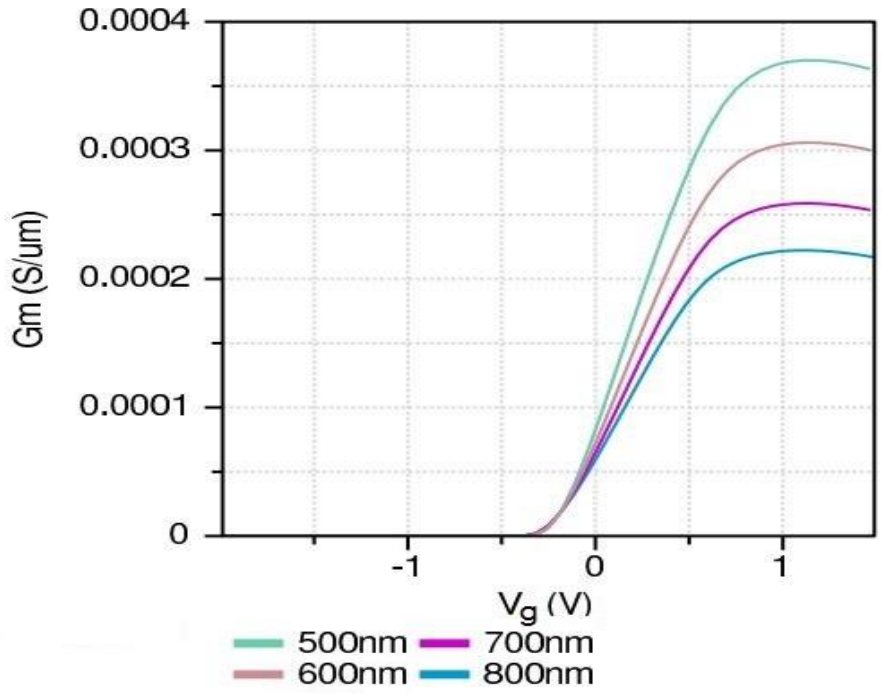

(b)

Fig. 40. (a) Transconductance vs. Gate Length for Si (b) Transconductance vs. Gate length for ZnO

In fig. 40(a) and fig. 40(b), with increase in gate length the transconductance for both nanowire FETs have decreased as expected [117]. Thus in all studies Si nanowire FET has shown higher transconductance than ZnO yielding higher gain and sensitivity.

7.6 Conclusion

In this study, various electrical properties of ZnO and Si nanowire long channel FETs were analyzed. Properties like subthreshold swing, threshold voltage and transconductance study were observed by varying temperature, channel diameter and gate length keeping all other parameters constant. At room temperature, the subthreshold swing of ZnO surpassed that of Si by a large margin deteriorating the device performance. The subthreshold swing of ZnO improved a little with increasing gate length and lowering diameter. Hence to implement faster device, Si is preferable.

The threshold voltage of Silicon and ZnO varied less with temperature, channel diameter and gate length. ZnO showed better threshold voltage value than Si. So ZnO provides an attractive choice for logic applications.

Again in case of transconductance, Si achieved better value than ZnO. For sensitive devices like biosensors, Si is still the better choice. ZnO has propitious characteristics in the area of nanobiosensing and optoelectronics because of its stability in air, chemical stability, ease of synthesis and nontoxicity. But significant amount of research is yet to be done for improving the performance of ZnO nanowire FET. The main problem still being faced with ZnO nanowire FETs is a need for stable, reproducible p-type doping of ZnO which has not been achieved until now.

REFERENCES

[1] V. Dzyadevych, V. N. Arkhypova, A. P. Soldatkin et al., “Amperometric enzyme biosensors: past, present and future Biocapteurs enzymatiques a transduction amperometrique: passe, present, futur”, *Intermediate-Range Ballistic Missile*, vol. 29, pp. 171–180, 2008.

[2] P. T. Kissinger, “Biosensors—a perspective,” *Biosensors and Bioelectronics*, vol. 20, no. 12, pp. 2512–2516, 2005.

[3] C. Jianrong, M. Yuqing, H. Nongyue, W. Xiaohua, and L. Sijiao, “Nanotechnology and biosensors,” *Biotechnology Advances*, vol. 22, no. 7, pp. 505–518, 2004.

[4] X. Su, F. T. Chew, and S. F. Y. Li, “Design and application of piezoelectric quartz crystal-based immunoassay,” *Analytical Sciences*, vol. 16, no. 2, pp. 107–114, 2000.

[5] T. Liu, J. Tang, and L. Jiang, “The enhancement effect of gold nanoparticles as a surface modifier on DNA sensor sensitivity,” *Biochemical and Biophysical Research Communications*, vol. 313, no. 1, pp. 3–7, 2004.

[6] J. Richardson, P. Hawkins, and R. Luxton, “The use of coated paramagnetic particles as a physical label in a magneto immuno assay,” *Biosensors and Bioelectronics*, vol. 16, no. 9–12, pp. 989–993, 2001.

[7] Y. R. Chemla, H. L. Grossman, Y. Poon et al., “Ultrasensitive magnetic biosensor for homogeneous immunoassay,” *Proceedings of the National Academy of Sciences of the United States of America*, vol. 97, no. 26, pp. 14268–14272, 2000.

[8] H. Cai, C. Xu, P. He, and Y. Fang, “Colloid Au-enhanced DNA immobilization for the electrochemical detection of sequence specifc DNA,” *Journal of Electroanalytical Chemistry*, vol. 510, no. 1-2, pp. 78–85, 2001.

[9] A. L. Crumbliss, S. C. Perine, J. Stonehuerner, K. R. Tubergen, J. Zhao, and R. W. Henkens, “Colloidal gold as a biocompatible immobilization matrix suitable for the fabrication of enzyme electrodes by electrodeposition,” *Biotechnology and Bioengineering*, vol. 40, no. 4, pp. 483–490, 1992.

[10] J. Zhao, J. P. O’Daly, R. W. Henkens, J. Stonehuerner, and A. L. Crumbliss, “A xanthine oxidase/colloidal gold enzyme electrode for amperometric biosensor applications,” *Biosensors and Bioelectronics*, vol. 11, no. 5, pp. 493–502, 1996.

[11] X. Xu, S. Liu, and H. Ju, “A novel hydrogen peroxide sensor via the direct electrochemistry of horseradish peroxidase immobilized on colloidal gold modifed screen-printed electrode,” *Sensors*, vol. 3, no. 9, pp. 350–360, 2003.

[12] M. L. Curri, A. Agostiano, G. Leo, A. Mallardi, P.Cosma, and M. Della Monica, “Development of a novel enzyme/semiconductor nanoparticles system for biosensor application,” *Materials Science and Engineering C*, vol. 22, no. 2, pp. 449–452, 2002.

[13] M. B. Gonzalez-Garcıa, C. Fernandez-Sanchez, and A. Costa-Garcıa, “Colloidal gold as an electrochemical label of streptavidin—biotin interaction,” *Biosensors and Bioelectronics*, vol. 15, no. 5-6, pp. 315–321, 2000.

[14] J. J. Davis, K. S. Coleman, B. R. Azamian, C. B. Bagshaw, and M. L. H. Green, “Chemical and biochemical sensing with modified single walled carbon nanotubes,” *Chemistry*, vol. 9, no. 16, pp. 3732–3739, 2003.

[15] S. Sotiropoulou, V. Gavalas, V. Vamvakaki, and N. A. Chaniotakis, “Novel carbon materials in biosensor systems,” *Biosensors and Bioelectronics*, vol. 18, no. 2-3, pp. 211–215, 2002.

[16] B. R. Azamian, J. J. Davis, K. S. Coleman, C. B. Bagshaw, and M. L. H. Green, “Bioelectrochemical single-walled carbon nanotubes,” *Journal of the American Chemical Society*, vol. 124, no. 43, pp. 12664–12665, 2002.

[17] A. Guiseppi-Elie, C. Lei, and R. H. Baughman, “Direct electron transfer of glucose oxidase on carbon nanotubes,” *Nanotechnology*, vol. 13, no. 5, pp. 559–564, 2002.

[18] J. Wang, “Carbon-nanotube based electrochemical biosensors: a review,” *Electroanalysis*, vol. 17, no. 1, pp. 7–14, 2005.

[19] Y. Cui and C. M. Lieber, “Functional nanoscale electronic devices assembled using silicon nanowire building blocks,” *Science*, vol. 291, no. 5505, pp. 851–853, 2001.

[20] J. Wang, “Electrochemical nucleic acid biosensors,” *Analytica Chimica Acta*, vol. 469, no. 1, pp. 63–71, 2002.

[21] B. M. Cullum, G. D. Grifin, G. H. Miller, and T. Vo-Dinh, “Intracellular measurements in mammary carcinoma cells using fiber-optic nanosensors,” *Analytical Biochemistry*,vol.277, no. 1, pp. 25–32, 2000.

[22] A. Umar, M.M. Rahman, A. Al-Hajry, and Y.-B.Hahn, “Highly sensitive cholesterol biosensor based on well-crystallized flower-shaped ZnO nanostructures,” *Talanta*, vol. 78, no. 1, pp. 284–289, 2009.

[23] S. Yang, “Nanowires and nanobelts, materials, properties and devices,” in *Nanowires and Nanobelts of Functional Materials*, Z. L. Wang, Ed., vol. 2, pp. 209–238, Kluwer Academic, New York, NY, USA, 2003.

[24] Y. Cui, Q. Wei, H. Park, and C. M. Lieber, “Nanowire nanosensors for highly sensitive and selective detection of biological and chemical species,” *Science*, vol. 293, no. 5533, pp. 1289–1292, 2001.

[25] B. Huang, F. Yu, and R. N. Zare, “Surface plasmon resonance imaging using a high numerical aperture microscope objective,” *Analytical Chemistry*, vol. 79, no. 7, pp. 2979–2983, 2007.

[26] E. Stern, J. F. Klemic, D. A. Routenberg et al., “Label free immuno detection with CMOS-compatible semiconducting nanowires,” *Nature*, vol. 445, no. 7127, pp. 519–522, 2007.

[27] Chen KI, Li BR, Chen YT. Silicon nanowire field-effect transistor-based biosensors for biomedical diagnosis and cellular recording investigation. Nano Today. 2011; 30; 6(2): 131-154.

[28] Li H, Yin Z, He Q, Li H, Huang X, Lu G, Fam DW, Tok AI, Zhang Q, Zhang H. Fabrication of Single and Multilayer MoS2 Film Based Field Effect Transistors for Sensing NO at Room Temperature. Small. 2012; 9; 8(1): 63-67.

[29] Zhou FS, Wei QH. Scaling laws for nanoFET sensors. Nanotechnology. 2008; 19(1): 015504.

[30] Li BR, Chen CC, Kumar UR, Chen YT. Advances in nanowire transistors for biological analysis and cellular investigation. Analyst. 2014; 139(7): 1589-1608.

[31] Heller I, Janssens AM, Männik J, Minot ED, Lemay SG, Dekker C. Identifying the mechanism of biosensing with carbon nanotube transistors. Nano Lett. 2008; 8(2): 591-595.

[32] Nair PR, Alam, MA, Screening-limited response of nanobiosensors. Nano Lett. 2008; 8(5): 1281-1285.

[33] Stern E, Wagner R, Sigworth FJ, Breaker R, Fahmy TM, Reed MA. Importance of the Debye screening length on nanowire field effect transistor sensors. Nano Lett. 2007; 7(11): 3405-3409.

[34] Tang X, Bansaruntip S, Nakayama N, Yenilmez E, Chang YL, Wang Q. Carbon nanotube DNA sensor and sensing mechanism. Nano Lett. 2006; 6(8): 1632-1636.

[35] Sarkar D, Liu W, Xie X, Anselmo AC, Mitragotri S, Banerjee K. MoS2 field-effect transistor for nextgeneration label-free biosensors. ACS Nano. 2014; 8(4): 3992-4003

[36] F. Patolsky, G.F. Zheng, C.M. Lieber, Nat. Protoc. 1 (2006) 1711

[37] B.Z. Tian, P. Xie, T.J. Kempa, D.C. Bell, C.M. Lieber, Nat. Nanotechnol. 4 (2009) 824.

[38] Y. Cui, X.F. Duan, J.T. Hu, C.M. Lieber, J. Phys. Chem. B 104 (2000) 5213.

[39] M.C. Lin, C.J. Chu, L.C. Tsai, H.Y. Lin, C.S. Wu, Y.P. Wu, Y.N. Wu, D.B. Shieh, Y.W. Su, C.D. Chen, Nano Lett. 7 (2007) 3656—3661

[40] E. Stern, J.F. Klemic, D.A. Routenberg, P.N. Wyrembak, D.B. Turner-Evans, A.D. Hamilton, D.A. LaVan, T.M. Fahmy, M.A. Reed, Nature 445 (2007) 519.

[41] Y.B. Zhang, Y. Xiong, X.A. Yang, Y. Wang, W.H. Han, F.H. Yang, J. Nanosci. Nanotechnol. 10 (2010) 7113—7116.

[42] S.P. Lin, C.Y. Pan, K.C. Tseng, M.C. Lin, C.D. Chen, C.C. Tsai, S.H. Yu, Y.C. Sun, T.W. Lin, Y.T. Chen, Nano Today 4 (2009) 235.

[43] T. Kudo, T. Kasama, T. Ikeda, Y. Hata, S. Tokonami, S. Yokoyama, T. Kikkawa, H. Sunami, T. Ishikawa, M. Suzuki, K. Okuyama, T. Tabei, K. Ohkura, Y. Kayaba, Y. Tanushi, Y. Amemiya, Y. Cho, T. Monzen, Y. Murakami, A. Kuroda, A. Nakajima, Jpn. J. Appl. Phys. 48 (2009).

[44] O. Knopfmacher, A. Tarasov, W.Y. Fu, M. Wipf, B. Niesen, M. Calame, C. Schonenberger, Nano Lett. 10 (2010) 2268— 2274.

[45] N. Elfstrom, R. Juhasz, I. Sychugov, T. Engfeldt, A.E. Karlstrom, J. Linnros, Nano Lett. 7 (2007) 2608.

[46] G. Pennelli, Microelectron. Eng. 86 (2009) 2139.

[47] X.T. Vu, J.F. Eschermann, R. Stockmann, R. Ghosh Moulick, A. Offenhausser, S. Ingebrandt, Phys. Status Solidi A 206 (2009) 426—434.

[48] R.S. Wagner, W.C. Ellis, Appl. Phys. Lett. 4 (1964) 89.

[49] Y. Wu, J. Xiang, C. Yang, W. Lu, C.M. Lieber, Nature 430 (2004) 61.

[50] W. Lu, C.M. Lieber, J. Phys. D: Appl. Phys. 39 (2006) R387

[51] Sarkar D, Liu W, Xie X, Anselmo AC, Mitragotri S, Banerjee K. MoS2 field-effect transistor for nextgeneration label-free biosensors. ACS Nano. 2014; 8(4): 3992-4003.

[52] Paul DR, Robeson LM. Polymer nanotechnology: nanocomposites. Polymer. 2008; 49(15):3187-3204.

[53] Hangarter CM, Bangar M, Mulchandani A, Myung NV. Conducting polymer nanowires for chemiresistive and FET-based bio/chemical sensors. J Mater Chem. 2010; 20 (16): 3131-3140.

[54] Mulchandani A, Myung NV. Conducting polymer nanowires-based label-free biosensors. Curr Opin Biotech. 2011; 22(4): 502-508.

[55] Li J, Duan Y, Hu H, Zhao Y, Wang Q. Flexible Nws sensors in polymer, metal oxide and semiconductor materials for chemical and biological detection. Sensor Actuate B Chem. 2015; 219: 65–82.

[56] Yang W, Ratinac KR, Ringer SP, Thordarson P, Gooding JJ, Braet F. Carbon nanomaterials in biosensors: should you use nanotubes or graphene?. Angew Chem Int Ed. 2010; 49(12): 2114-2138.

[57] Makowski M S, Ivanisevic A. Molecular Analysis of Blood with Micro-/Nanoscale Field Effect-Transistor Biosensors. Small. 2011; 7: 1863–1875.

[58] Ohno Y, Maehashi K, Matsumoto K. Label-free biosensors based on aptamer-modified graphene field-effect transistors. J am Chem Soc. 2010; 132(51): 18012-18013

[59] W. Lu, C.M. Lieber, J. Phys. D: Appl. Phys. 39 (2006) R387.

[60] Y. Huang, X.F. Duan, Q.Q. Wei, C.M. Lieber, Science 291 (2001) 630.

[61] D. Whang, S. Jin, Y. Wu, C.M. Lieber, Nano Lett. 3 (2003) 1255.

[62] S. Jin, D.M. Whang, M.C. McAlpine, R.S. Friedman, Y. Wu, C.M. Lieber, Nano Lett. 4 (2004) 915.

[63] X.L. Li, L. Zhang, X.R. Wang, I. Shimoyama, X.M. Sun, W.S. Seo, H.J. Dai, J. Am. Chem. Soc. 129 (2007) 4890.

[64] A. Tao, F. Kim, C. Hess, J. Goldberger, R.R. He, Y.G. Sun, Y.N. Xia, P.D. Yang, Nano Lett. 3 (2003) 1229.

[65] G.H. Yu, A.Y. Cao, C.M. Lieber, Nat. Nanotechnol. 2 (2007) 372.

[66] E.M. Freer, O. Grachev, D.P. Stumbo, Nat. Nanotechnol. 5 (2010) 525.

[67] L.F. Dong, J. Bush, V. Chirayos, R. Solanki, J. Jiao, Nano Lett. 5 (2005) 2112.

[68] A. Motayed, M.Q. He, A.V. Davydov, J. Melngailis, S.N. Mohammad, J. Appl. Phys. 100 (2006) 114310.

[69] S. Raychaudhuri, S.A. Dayeh, D.L. Wang, E.T. Yu, Nano Lett. 9 (2009) 2260.

[70] Z.Y. Fan, J.C. Ho, Z.A. Jacobson, R. Yerushalmi, R.L. Alley, H. Razavi, A. Javey, Nano Lett. 8 (2008) 20.

[71] R. Yerushalmi, Z.A. Jacobson, J.C. Ho, Z. Fan, A. Javey, Appl. Phys. Lett. 91 (2007) 203104.

[72] Y.K. Chang, F.C.N. Hong, Nanotechnology 20 (2009) 195302

[73] Y.K. Kim, P.S. Kang, D.I. Kim, G. Shin, G.T. Kim, J.S. Ha, Small 5 (2009) 727.

[74] M. Bohr, S.U. Ahmed, L. Brigham, R. Chau, R. Gasser, R. Green, W. Hargrove, E. Lee, R. Natter, S. Thompson, K. Weldon and S. Yang, IEDM Technical Digest, p. 273, 1994

[75] Scott Thompson, Paul Packan, Mark Bohr, Intel Technology Journal (1998).

[76] M. Bescond, K. Nehari, J. L. Autran, N. Cavassilas, D. Munteanu and M. Lannoo, IEDM Tech Digest (IEEE), San Francisco (USA), p. 617, (2004).

[77] R. V. Martínez, J. Martínez, and R. Garcia, *Nanotechnology* 21, 24(2010).

[78] K. Nehari, N. Cavassilas, J. L. Autran, M. Bescond, D. Munteanu and M. Lannoo, *Proceedings of 35th European Solid-State Device Research Conference,* p. 229 *(ESSDERC 2005).*

[79] U. Oezguer, Y.I. Alivov, C. Liu, A. Teke, M.A. Reshchikov, S. Dogan, V. Avrutin,S.J. Cho, and H. Morkoc. A comprehensive review of ZnO materials and devices. Journal of Applied Physics, 98:041301, (2005).

[80] Klingshirn, J. Fallert, H. Zhou, J. Sartor, C. Thiele, F. Maier-Flaig, D. Schneider, and H. Kalt. 65 years of ZnO research - old and very recent results. physica status solidi (b), 247(6):1424-1447, (2010).

[81] Chattopadhyay, Soubhik et al. "Optical Property Modification Of Zno: Effect Of 1.2 Mev Ar Irradiation". physica status solidi (c) 8.2 (2010): 512-515.Anderson Janotti and Chris G Van de Walle, Fundamentals of zinc oxide as a semiconductor, Rep. Prog. Phys. 72**,** 126501 (29pp), (2009)

[82] M. Grundmann, H. Frenzel, A. Lajn, M. Lorenz, F. Schein and H. von Wenckstern.Transparent semiconducting oxides: materials and devices. physica status solidi (a),207(6):1437-1449, (2010).

[83] M. Law, L.E. Greene, J.C. Johnson, R. Saykally, and P. Yang. Nanowire dyesensitized solar cells. Nature Materials, 4(6):455-459, (2005).

[84] P. Ravirajan, A.M. Peiro, M.K. Nazeeruddin, M. Graetzel, D.D.C. Bradley, J.R.Durrant, and J. Nelson. Hybrid polymer/zinc oxide photovoltaic devices with

vertically oriented ZnO nanorods and an amphiphilic molecular interface layer. The Journal of Physical Chemistry B, 110(15):7635-7639, (2006).

[85] J. S. Kim, W. I. Park, C.-H. Lee, and G.-C. Yi, ZnO nanorod biosensor for highly sensitive detection of specific protein binding,[J. Korean Phys. Soc., vol. 49, pp. 1635–1639, (2006).

[86] P. D. Batista and M. Mulato, BZnO extended-gate field-effect transistors as pH sensors,[Appl. Phys. Lett., vol. 87, pp. 143508-1–143508-3, (2005).

[87] B. S. Kang, F. Ren, Y. W. Heo, L. C. Tien, D. P. Norton, and S. J. Pearton, pH measurements with single ZnO nanorods integrated with a microchannel,[Appl. Phys. Lett., vol. 86, pp. 112105-1–112105-1,(2005).

[88] O. Dulub, B. Meyer, and U. Diebold, Observation of the dynamical change in a water monolayer adsorbed on a ZnO surface,[Phys. Rev. Lett., vol. 95, pp. 136101-1–136101-4, (2005).

[89] S. M. Al-Hillia, M. Willander, A. O ¨st, and P. Stra˚lfors, ZnO nanorods as an intracellular sensor for pH measurements, [J. Appl. Phys., vol. 102, pp. 084304-1–084304-5, (2007).

[90] S. M. Al-Hilli, R. T. Al-Mofarji, and M. Willander, BZinc oxide nanorod for intracellular pH sensing,[Appl. Phys. Lett.,vol. 89, pp. 173119-1–173119-3, (2006).

[91] Fulati A, Ali SMU, Asif MH, Alvi NH, Willander M, Brännmark C, Stralfors P,Börjesson SI, Elinder F, Danielsson B: An intracellular glucose biosensorbased on nanoflake ZnO. Sens Actuators B, 150:673-680, (2010).

[92] Ali SMU, Alvi NH, Ibupoto Z, Nur O, Willander M, Danielsson B: Selective potentiometric determination of uric acid with uricase immobilized on ZnO nanowires. Sens Actuators B,152:241-247, (2011)

[93] Lin SS, Chen IC, Yang J, Hsueh TJ, Hsu CL, Lee HE, Shieh TY: A study on one-step immobilization of horse immunoglobulin with vertically grown ZnO nanorods substrates. J Electrochem Soc, 158:K107-K111, (2011).

[94] Choi A, Kim K, Jung HI, Lee SY: ZnO nanowire biosensors for detection of biomolecular interactions in enhancement mode. Sens Actuators B,148:577-582,(2010).

[95] Pei Lin, X. Yan, Z. Kang, Y. Zhao, Y. Lei, C. Li,H. Du, Y. Zhang, Enzyme-coated single ZnO nanowire FET biosensor for detection of uric acid, Sensors and Actuators B: Chemical (2010).

[96] Niepelt, Raphael et al. "Biofunctionalization Of Zinc Oxide Nanowires For DNA Sensory Applications". Nanoscale Res Lett 6.1 (2011): 511.

[97] Cui Y, Wei Q, Park H, Lieber CM: Nanowire nanosensors for highly sensitive and selective detection of biological and chemical species, Science 2001, 293:1289-1292.

[98] Patolsky F, Timko BP, Zheng G, Lieber CM: Nanowire-based nanoelectronic devices in the life sciences. MRS Bull, 32:142-149, (2007).

[99] Cattani-Scholz A, Pedone D, Dubey M, Neppl S, Nickel B, Feulner P, Schwartz J, Abstreiter G, Tornow M: Organophosphonate-based PNA functionalization of silicon nanowires for label-free DNA detection. ACSNano, 2:1653-1660, (2008).

[100] Singh, Pradyumna S. "From Sensors To Systems: CMOS-Integrated Electrochemical Biosensors". IEEE Access 3 (2015): 249-259.

[101] Zhou J, Xhu NS, Wang ZL: Dissolving behavior and stability of ZnO wires in biofluids: a study on biodegradability and biocompatibility of ZnO nanostructures. Adv Mater, 18:2432-2435, (2006).

[102] Cheng C, Xin R, Leng Y, Yu D, Wang N: Chemical stability of ZnO nanostructures in simulated physiological environments and its application in determining polar directions. Inorg Chem,47:7868-7873, (2008).

[103] Israr MQ, Sadaf JR, Nur O, Willander M, Salman S, Danielsson B: Chemically fashioned ZnO nanowalls and their potential application for potentiometric cholesterol biosensor. Appl Phys Lett, 98:253705, (2011).

[104] https://nanohub.org/tools/nanofinfet

[105] T. Mikolajick, Thomas and Walter M. Weber. "Silicon Nanowires: Fabrication And Applications". Anisotropic Nanomaterials (2015): 1-25.

[106] B. P. Haley, S. Lee, M. Luisier, H. Ryu, F. Saied, S. Clark, H. Bae, and G. Klimeck, *Journal of Physics: Conference Series* 180, 012075, (2009).

[107] Tawseef A. Bhat, M. Mustafa and M.R. Beigh, Study of Short Channel Effects in n-FinFET Structure for Si, GaAs, GaSb and GaN Channel Materials, Journal of nano- and electronic physics Vol. 7 No 3, 03010(5pp) (2015).

[108] S. N. Cha et al., APPLIED PHYSICS LETTERS **89**, 263102, (2006)

[109] Hanada T,Basic Properties of ZnO, GaN, and Related Materials. American Scientific Publishers 1: 1-18, (2009).

[110] Jackson, Kenneth A., and W. Schröter. Handbook of Semiconductor Technology. Weinheim: Wiley-VCH, 2000.

[111] https://en.wikipedia.org/wiki/Effective_mass_(solid-state_physics)

[112] Bertazzi, F., Goano, M. & Bellotti, E. Journal of Elec Materi (2007) 36: 857.

[113] https://en.wikipedia.org/wiki/Zinc_oxide

[114] H. Arabshahi, F. Badieian-Baghsiyahi, Simulation of High Field Electron Transport in Wurtzite Phase of ZnO, International Archive of Applied Sciences and Technology, Volume 3: 105 – 111, (March 2012).

[115] S. N. Cha et al, High performance ZnO nanowire field effect transistor, IEEE Xplore,(2005).

[116] Hong, Woong-Ki et al. "Electrical Properties Of Zno Nanowire Field Effect Transistors By Surface Passivation". Colloids and Surfaces A: Physicochemical and Engineering Aspects 313-314 (2008): 378-382.

[117] Li, J. et al. "Advanced Performance And Scalability Of Si Nanowire Field-Effect Transistors Analyzed Using Noise Spectroscopy And Gamma Radiation Techniques". J. Appl. Phys. 114.20 (2013): 203704